Developing a synergistic combination of an anti-inflammatory compound and a broad-range antibiotic as an effective therapy for sepsis

M.Sc. Thesis

By

Rahul Sharma

BIOSCIENCES AND BIOMEDICAL ENGINEERING

INDIAN INSTITUTE OF TECHNOLOGY INDORE

May 2023

Developing a synergistic combination of an anti-inflammatory compound and a broad-range antibiotic as an effective therapy for sepsis

A THESIS

Submitted in partial fulfillment of the

requirements for the award of the degree

of

Master of Science

by

Rahul Sharma

BIOSCIENCES AND BIOMEDICAL ENGINEERING

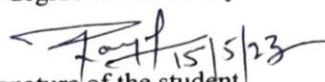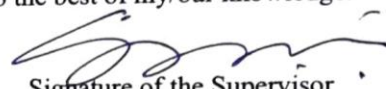# INDIAN INSTITUTE OF TECHNOLOGY INDORE

May 2023

INDIAN INSTITUTE OF TECHNOLOGY INDORE

CANDIDATE'S DECLARATION

I hereby certify that the work which is being presented in the thesis entitled **"Developing a synergistic combination of an anti-inflammatory compound and a broad-range antibiotic as an effective therapy for sepsis"** in the partial fulfillment of the requirements for the award of the degree **of MASTER OF SCIENCE** and submitted in the **DEPARTMENT OF BIOSCIENCES AND BIOMEDICAL ENGINEERING, Indian Institute of Technology Indore,** is an authentic record of my own work carried out during the period from Aug 2021 to May 2023. Thesis submission under the supervision of Dr. Mirza S. Baig, Associate professor, IIT Indore. The matter presented in this thesis has not been submitted by me for the award of any other degree of this or any other institute.

15|5|23

Signature of the student

(Rahul Sharma)

This is to certify that the above statement made by the candidate is correct to the best of my/our knowledge.

Signature of the Supervisor

(Dr. Mirza S. Baig)

17.05.2023

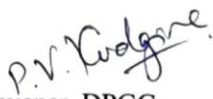---

Rahul Sharma has successfully given his/her M.Sc. Oral Examination held on **May 8, 2023**.

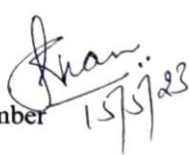Signature of Supervisor of MSc thesis

(Dr. Mirza S. Baig)

Date:

Signature of PSPC Member

(Dr. Hem Chandra Jha)

Convener, DPGC

(Prof. Prashant Kodgire)

Date:

Signature of PSPC Member   15/5/23

(Dr. Kiran Bala)

----

i

ACKNOWLEDGEMENTS

Dedicated

To

My Parents

and

My Family

Abstract

Sepsis is a multi-organ dysfunction condition brought on by uncontrolled inflammation after a pathogenic infection. The pathogen or cytokines are first released into the bloodstream by diseased or injured tissue. The blood contains a range of cells that might induce inflammation, such as neutrophils, natural killer cells, and, most notably, macrophages. The proposed therapeutic strategy against sepsis is based on a novel drug combination. We propose a novel synergistic combination of a broad-spectrum antibiotic and repurposed anti-inflammatory drug Repurposed Drug. Antibiotic not only can kill a broad range of bacterial species but could also control chronic inflammation in the host by preventing the activation of TIRAP, which is necessary for the induction of key inflammatory signaling events. In our previous studies, Repurposed Drug has already been repurposed to target TIRAP and inhibit its activation. Our in vivo studies not only suggest but validate our hypothesis that combined Antibiotic and Repurposed Drug preparation shows high potency in a septic mouse model. This novel combination therapy is a promising strategy for the treatment of severe sepsis.

LIST OF PUBLICATIONS

1. *Rajat Atre [1†] , **Rahul Sharma [1†]** , Alexander G Obukhov [2,3] , Uzma Saqib [4] ,Sadiq Umar [5] , Gajanan N Darwhekar [6] , Mirza S Baig [1], *.* An improved mouse model of sepsis based on intraperitoneal injections of the enriched culture of cecum slurry. doi: *https://doi.org/10.1101/2023.04.06.535817* (**Preprinted- bioRxiv and under review in JMIRxMED, Impact factor- 7.8).**
    † = equal authorship

2. *Rajat Atre [a 1], **Rahul Sharma [a 1]**, Gaponenko Vadim [b], Kundan Sola nki [a], Khandu Wadhonkar [a], Neha Singh [a], Pramod Patidar [a], Rakhi Khabiya [a c], Harshita Samaur [a], Sreeparna Banerjee [d], Mirza S. Baig [a].* The indispensability of Macrophage Adaptor Proteins in Chronic Inflammatory Diseases. doi https://doi.org/10.1016/j.intimp.2023.110176 , Volume 119, June 2023, 110176. (**International Immunopharmocology, Impact factor-5.7**).
    1 = equal authorship

3. *Solanki K, Atre R, **Sharma R**, Bezsonov E, Baig MS.* Small Molecule Inhibitors Targeting Endothelial IL-1βReceptor (IL-1R1): A Novel Approach to Atherosclerosis Therapy. Austin J Pharmacol Ther. 2023; 11(1): 1170. (**Austin journal of pharmacology, Impact factor-2.8**)

4. Novel synergistic combination therapy for the treatment of sepsis (**Patent under process**)

x

TABLE OF CONTENTS

LIST OF FIGURES

1. Chapter1

1.1. Introduction

Fig. 1.1.1.1: Schematic representation of sepsis progression after bacterial infection. Bacteria leads to chronic inflammation via stimulating various immune cells which further led to multi-organ damage.............................. 1

Fig. 1.1.1.2: Diagrammatic representation of progression of sepsis where from all septic patients 50-60% progress to severe sepsis and for that 20-30% progress to life threatening septic shock...**2**

Fig. 1.1.1.3: Epidemiology of sepsis is most prevalent in South America, Africa, and the Indian subcontinent. **3**

Fig. 1.1.2.1: A graph showing the mortality rate in septic patients where red bar indicates the mortality in the patients with pathogen in their blood, and blue bar indicates the mortality in the patients with no pathogen in their blood. **4**

Fig. 1.1.2.2: The bar graph showing mortality rate in the septic patients with different bacterial species isolated from their blood. This indicates the potential of different bacterial species to cause mortality by inducing sepsis. **5**

Fig. 1.1.3.1: Diagrammatic representation of the molecular signalling stimulated by LPS. **7**

LIST OF TABLES

Chapter5

ABBREVIATIONS

RD	Repurposed Drug
Ab	Antibiotic
H&E	Hematoxylin and Eosin
BTK	Bruton's Tyrosine Kinase
PKCδ	Protein Kinase C delta
SIRS	Systemic inflammatory response syndrome
LPS	Lipopolysaccharide
ICU	Intensive care unit
MyD88	Myeloid differentiation primary response 88
TIRAP	Toll-interleukin-1 Receptor (TIR) domain-containing adaptor protein
TRAF-6	TNF Receptor Associated Factor 6
AP1	Activator protein 1
NFkB	Nuclear factor kappa-light-chain enhancer
SDS	Sodium dodecyl sulphate-polyacrylamide gel electrophoresis
RT-PCR	Reverse Transcription-Polymerase Chain Reaction
MD simulations	Molecular Dynamic simulations
IL-12	Interleukin-12
IL-23	Interleukin-23
CS	Cecal slurry
Gram -ve	Gram negative
Gram +ve	Gram positive
TNF-α	Tumor necrosis factor alpha
FDA	Food and Drug Administration

NOMENCLATURE

ml   millilitre

mM   millimolar

ng   nanogram

nM   nanomolar

ns   nanosecond

μL   microlitre

μM   micro-molar

^{o}C degree centigrade

1. Chapter1

1.1. Introduction

1.1.1. Sepsis

Sepsis is a potentially fatal organ dysfunction syndrome that results from an uncontrolled and dysregulated host immunological response to any infection or damage (Singer et al., 2016).
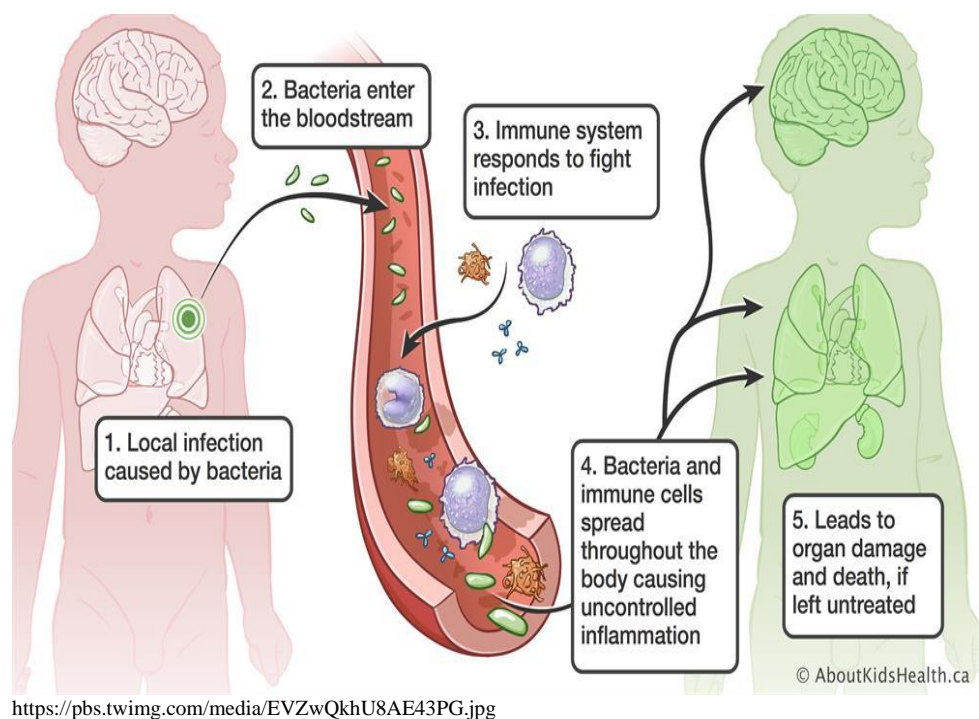
Fig. 1.1.1.1: A diagram depicting the course of sepsis following bacterial infection. Bacteria cause persistent inflammation by stimulating multiple immune cells, resulting in multi-organ damage.

A multitude of injuries or diseases can result in sepsis. The pathogen or cytokines are first released into the bloodstream by diseased or injured tissue. The blood contains a range of cells that might induce inflammation, such as neutrophils, natural killer cells, and, most notably, macrophages (Shalova et al., 2015). Infections, cytokines, and inflammatory cells

then spread to other organs, where they cause inflammation. If this reaction continues for an extended period, sepsis, a condition characterized by persistent inflammation and a variety of abnormalities, develops (**Fig. 1.1.1.1**).. When persistent inflammation is not treated for an extended period, an illness known as severe sepsis develops (Bosmann & Ward, 2013). This causes a variety of organ malfunctions. This can be detected by a variety of obvious signs and symptoms, including an increase in heart rate, high blood sugar, a decrease in urine, an increase in breathing rate, and confusion. Furthermore, if left untreated, it resulted in septic shock, a cardiovascular malfunction (Angus & van der Poll, 2013). As the disease progresses, three major conditions might be noticed. SIRS is characterized by a high or low body temperature, a fast pulse, and an elevated respiratory rate (Ward & Gao, 2009). Sepsis involves the presence of two symptoms as well as a bodily infection. Severe sepsis is distinguished by the presence of hypotension or hypoperfusion in addition to sepsis. At this time, we can witness low blood platelet counts, breathing issues, decreased urine production, stomach discomfort, and changes in mental health. The presence of hypotension and an increase in lactate levels indicates septic shock (**Fig. 1.1.1.2**). It is the most lethal stage, with a mortality rate of more than 60% (Iscimen et al., 2008).
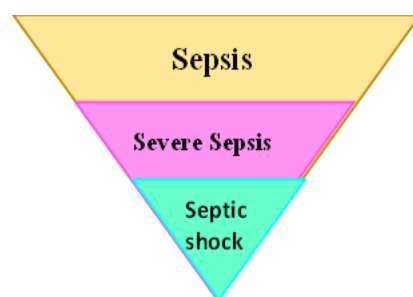
Fig. 1.1.1.2: Diagrammatic illustration of sepsis development in which 50-60% of sick patients progress to severe sepsis and 20-30% progress to life-threatening septic shock.

Sepsis is found across the world, but it is most common in South America, Africa, and the Indian subcontinent (**Fig. 1.1.1.3**) (Rudd et al., 2020). There is also a mortality rate of 40-80% (Vincent et al., 2019a). A number of medicines are available to eliminate the pathogen, provide supportive care, and assist the host in recovering from continuous organ damage caused by chronic inflammation. Antimicrobial therapy can be performed by either delivering a broad-spectrum antibiotic or administering a number of antibiotics. Ventilation should be included in supportive care to ensure an appropriate supply of oxygen. Erythrocyte transfusion is an option in extreme circumstances. Antibodies can suppress inflammatory mediators such as cytokines and endotoxins (LPS) (Bernard & Bernard, 2012). One is the suppression of inflammatory mediators such as cytokines and endotoxins (LPS) by antibodies or other mechanisms such as insulin, which boosts LDL cholesterol (bradley, 2023). Despite the availability of these medications, the death rate remains high. As a result, a new approach can be proposed (Jarczak et al., 2021a).
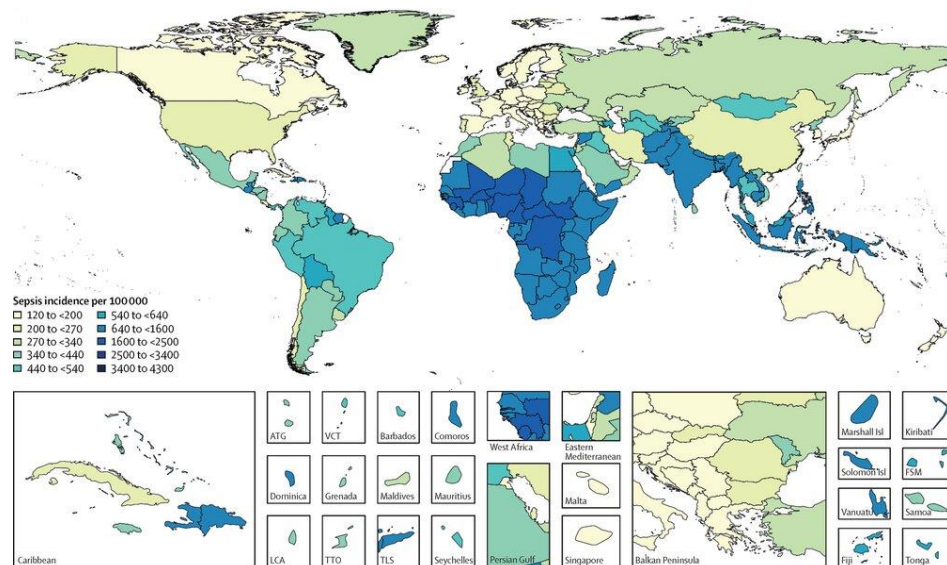
K. E. Rudd et al., "Global, regional, and national sepsis incidence and mortality, 1990–2017: analysis for the Global Burden of Disease Study," The Lancet, vol. 395, no. 10219, pp. 200–211, Jan. 2020, doi: 10.1016/S0140-6736(19)32989-7.

Fig. 1.1.1.3: Epidemiology: Sepsis is most prevalent in South America, Africa, and the Indian subcontinent.

1.1.2. Combination Therapy

Combination therapy is a method of treating an ailment by combining two or more treatments. Combination therapy is the use of two or more treatments or medications in conjunction to create a more effective therapeutic impact than would be gained by utilizing each treatment or medication alone. Combination therapy seeks to maximize treatment efficacy while minimizing negative effects and potential drug interactions.
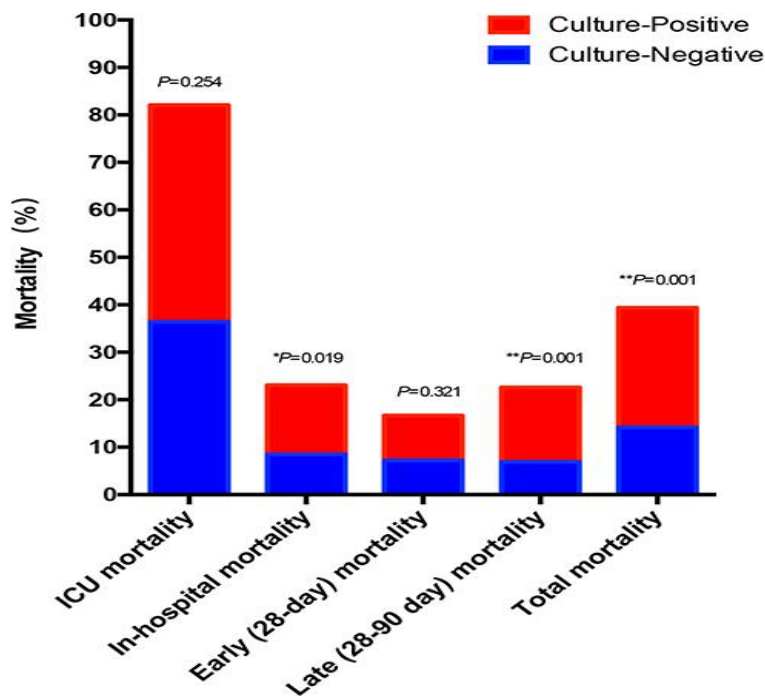
Polat G, Ugan RA, Cadirci E, Halici Z. Sepsis and Septic Shock: Current Treatment Strategies and New Approaches. Eurasian J Med. 2017 Feb;49(1):53-58. doi: 10.5152/eurasianjmed.2017.17062. PMID: 28416934; PMCID: PMC5389495.

Fig. 1.1.2.1: The graph depicting the death rate in septic patients, with the red bar representing mortality in patients with pathogens in their blood and the blue bar representing mortality in patients without pathogens in their blood.

According to one study, individuals in the ICU with infections in their blood died at a rate of over 80%, whereas those without pathogens died at a rate of around 40% (**Fig. 1.1.2.1**) (Vincent et al., 2019b), (Polat et al., 2017a). This could be because the endotoxins generated by the infections are still present in the body. As a result, we can conclude that mortality is caused by both pathogenic infection and dysregulated immune response.

In another investigation, we discovered that gram-negative bacteria are the top cause of death among all infections that cause sepsis (**Fig. 1.1.2.2**). There is also mortality caused by gram-positive bacteria, but it is not as severe (Polat et al., 2017b). Thus, targeting gram-negative induced inflammatory signaling in addition to killing a wide range of bacteria may be a more effective therapeutic strategy to treat sepsis.
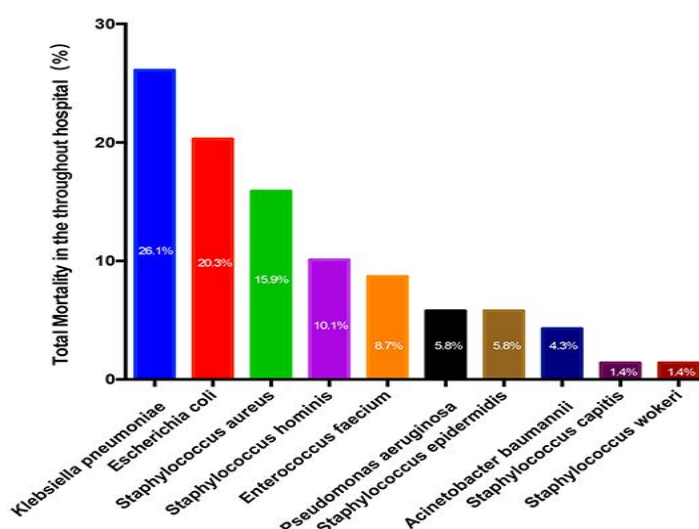
Polat G, Ugan RA, Cadirci E, Halici Z. Sepsis and Septic Shock: Current Treatment Strategies and New Approaches. Eurasian J Med. 2017 Feb;49(1):53-58. doi: 10.5152/eurasianjmed.2017.17062. PMID: 28416934; PMCID: PMC5389495.

Fig. 1.1.2.2: The bar graph depicts the mortality rate in septic patients with various bacterial species isolated from their blood. This suggests that different bacterial species have the capacity to cause death via producing sepsis. Gram-negative bacteria are shown to cause more adverse effects.

1.1.3. Scope and plan of the thesis-

The goal of this thesis is to create a potential therapeutic method for chronic inflammatory disorders, particularly sepsis. Although various therapies are currently available, they are not having much of an impact because the mortality rate remains between 40 and 80% (Polat et al., 2017c). As a result, in order to develop a better therapeutic, the mechanism underlying disease progression should be investigated further.

According to many research, the mortality in septic patients is caused not only by pathogenic invasion but also by a dysregulated immune response (Jarczak et al., 2021b). To treat the condition, eradicating germs is not enough; we must also restore the patient by lowering the inflammatory reaction. As a result, we chose combination therapy, which combines an antibiotic with an anti-inflammatory drug. The anti-inflammatory target we chose was likewise novel: TIRAP, which has only been shown to be implicated in inflammatory signaling. According to one study, gram-negative bacteria are the most common pathogen involved in the death of septic patients. As a result, we intended to focus on gam-negative bacteria-mediated inflammatory signaling, in which LPS is a major stimulant. The primary receptor involved in LPS-stimulated signaling in gram-negative bacteria is TLR4, which triggered the transcriptional factors NFkB and AP1, which in turn activated the genes responsible for pro-inflammatory cytokine production. The signaling molecules implicated are TRAF-6, MAPK, and other adaptors such as TIRAP and MyD88 ((Rajpoot et al., 2021a)). TIRAP is the most upstream of them, becoming active after interacting with and being phosphorylated by BTK and PKC**δ** tyrosine kinases, causing MyD88 to become active (**Fig. 1.3.1**). Because TIRAP may interact with BTK, and PKC**δ**, if we can break this link, we will be able to completely block TIRAP-mediated inflammatory signaling (**Fig. 1.3.2**). As a result, we were excited to find the TIRAP interaction site with these three compounds.
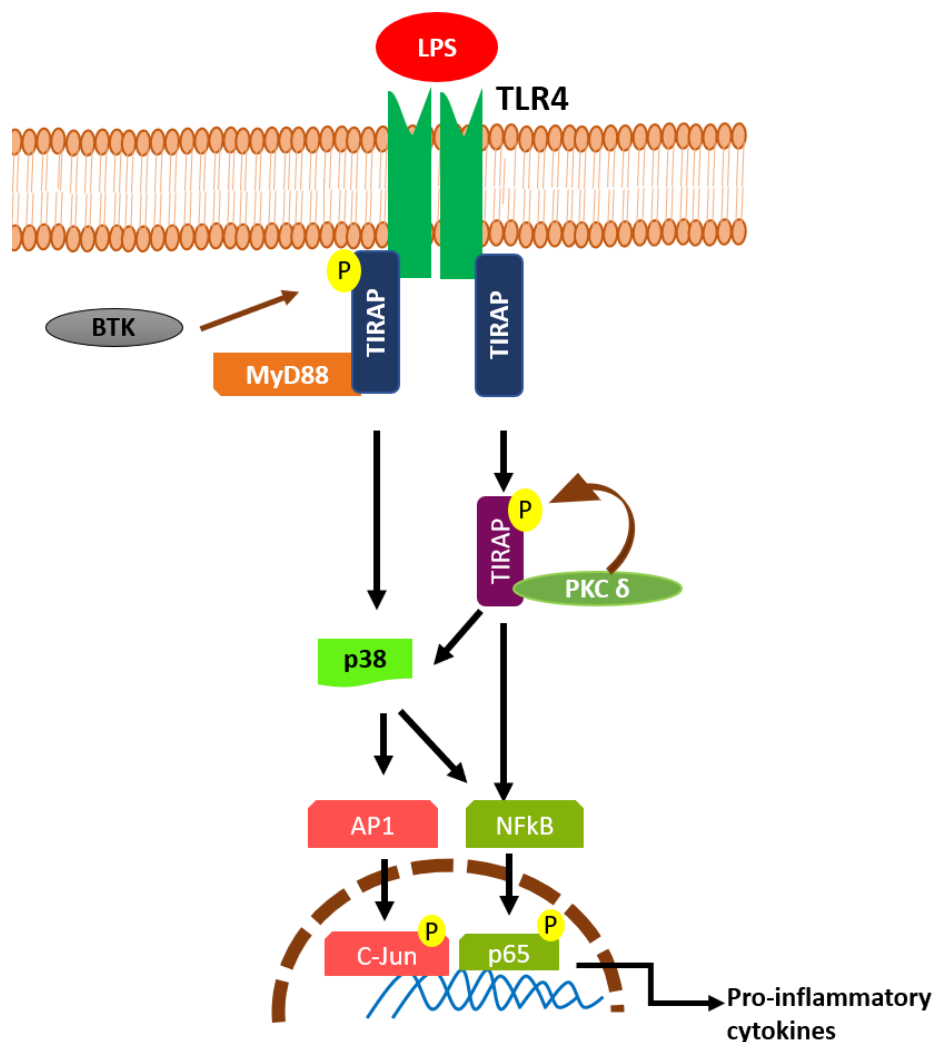
Fig. 1.1.3.1: Schematic representation of the molecular signalling stimulated by LPS.

Interestingly, TIRAP was found to share some common residues while interacting with all the three molecules. So, targeting that site is found to be a better and more efficient strategy to block the inflammatory signaling. In this study, we proposed a novel and better therapeutic strategy to treat the life-threatening sepsis. Broadly, following aims are covered in this thesis:
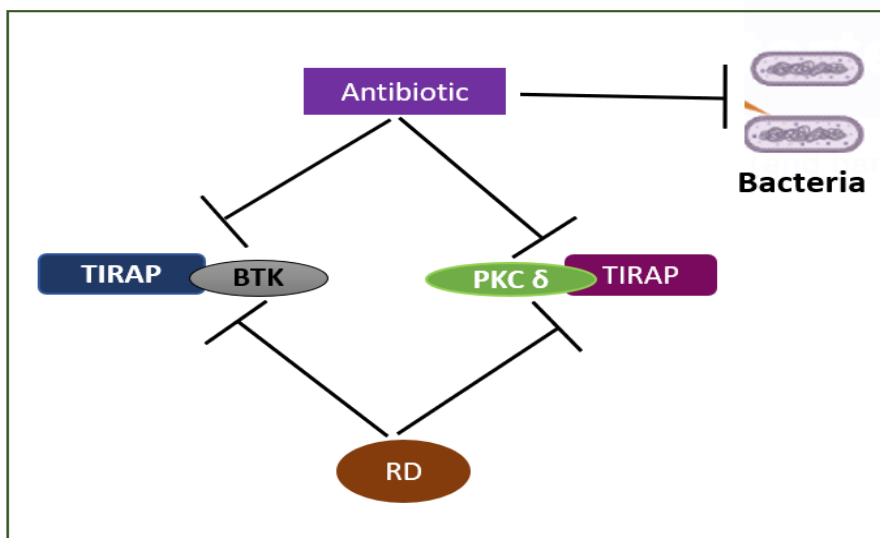
Fig. 1.1.3.2: Diagram showing combination therapy approach to target TIRAP.

1.1.3.1. To identify the interphase of TIRAP-BTK, and TIRAP-PKCδ : In this aim, we will identify the TIRAP binding site with BTK, and PKCδ by the molecular docking and MD simulation studies.

1.1.3.2. To identify drug targeting TIRAP: In this aim, we will screen the drug targeting at the TIRAP binding site for BTK, and PKCδ and will validate the anti-inflammatory effect through in vitro and in vivo study.

1.1.3.3. To identify antibiotic targeting TIRAP: In this aim, we will screen antibiotic targeting TIRAP binding site for BTK, PKCδ and validate its anti-inflammatory effect in vitro.

1.1.3.4. To design novel combination to treat sepsis: In this aim, we will study the synergistic in vivo effect of the combined drug by analyzing the survival rate and the affected organ morphology along with the biomarkers specific for sepsis.

2. Chapter 2

2.1. Materials and Methods

2.1.1. Molecular docking

AutoDock Vina and Schrodinger software were utilized to analyze protein-drug interactions, where blind docking of an FDA-approved library with the TIR domain of TIRAP (3UB2) was done and the initial pose from both platforms was analyzed. Polar ligands are favored at polar hotspots (such as hydrogen bond donors or acceptors) whereas non-polar ligands are preferred at non-polar hotspots (such as carbon atoms) (Parry et al., 1976a).

2.1.2. Cell culture

Mouse macrophages: RAW 264.7 was purchased from the National Centre for Cell Science (NCCS), Pune, India. These were cultured in DMEM (Dulbecco's minimal essential medium) supplemented with 10% heat inactivated Fetal Bovine Serum (FBS) and 1% antibiotic (penicillin and streptomycin).

2.1.3. Immunoblotting

Western blotting, used to separate and analyze protein macromolecules on the size basis, was first introduced by Towbin, et al. (*Towbin, H. (2009). Origins of Protein Blotting. Protein Blotting and Detection, Springer: 1-3*, n.d.). In this, the treated cells were washed with 1xPBS first and then lysed with RIPA buffer (Catalogue no. 89900, Thermo Fisher Scientific) which also contain protease and phosphatase inhibitor (Catalogue no. 88669, Thermo Fisher Scientific, M.A., U.S.). Then, the cells were crushed by using inverted

tip (on ice) and then the MCTs containing respective lysed samples were centrifuged at 13000 RPM for 30 mins at 4 degrees Celsius. After that, supernatant is collected in fresh chilled MCT and protein concentration was estimated with Bradford reagent (Catalogue No. 500-0006, Bio-Rad). Protein sample (70 ug) was then prepared with 4x lamillei blue dye containing b-mercaptoethanol in 1/10 of total dye. Sample was loaded along with the molecular marker (Catalogue No. 161-0394, Bio-Rad) in 10-12% SDS PAGE. And was transferred to PVDF membrane. The transfer was confirmed by visualizing with Ponceau stain. Then, after washing with 1x TBST (20 mM Tris–HCl, 500 mM NaCl, and 0.1% Tween 20) 3 times, 5 mins each, the membrane was blocked with 5% non-fat skimmed milk (Catalogue No. 170-6404, Bio-Rad) in 1x TBST. Then, excessive milk was removed by washing with TBST 3 times. The membrane was then probed with specific primary antibody for the interested protein with dilution 1:1000. The membrane was incubated for overnight at 4 degrees Celsius. After removing excess of antibody by washing, membranes were incubated with diluted horseradish-peroxidase (HRP) conjugated secondary antibodies with dilution 1:5000 at room temperature for 1 hour. Chemiluminescent substrate detection kit (Catalogue No. 1068701, Serva) was used to detect protein antibody complexes, and images were captured by the gel doc machine (LAS500). ImageJ software was used to quantify the images.

2.1.1. Real-Time Quantitative PCR

RT-PCR works based on the fluorescent reporter assay where the intensity of a fluorescent signal is generated by an intercalating dye during the amplification of target sequence and the number of PCR cycle upto which fluorescent signal is noticeable is called CT value. The CT value can be compared after subtracting and normalizing with the house keeping gene CT value and the one cycle decrease can be related to the double of target

sequence. This can be expressed as $2^{-\Delta CT}$. The values can be plotted and unknown target amount can be interpolated.

For the present study, RAW 264.7 mouse macrophages were cultured in 12 well plate and treated with LPS and drug (15 mins prior) at particular time point. After treatment, cells were washed with 1X PBS and then RNAiso Plus reagent (Takara Bio Inc.) was added and RNA isolation was performed according to the manufacturer instructions. To determine the purity and concentration of the extracted RNA, the ratio of absorbance readings at wavelengths 260 nm and 280 nm (A260/A280) was calculated. Total RNA (1 μg) was reverse transcribed (RT) using the Takara cDNA Synthesis Kit, according to the manufacturer's specifications. SYBR® Select Master Mix was used for the purpose of Real Time PCR in StepOnePlus Real-Time PCR Systems (AppliedBiosystems). The primer sets used are described in **Table 5.1.**

2.1.2. Immunofluorescence

In 12-well culture plates, 1* 104 cells per well were cultivated on coverslips (18 mm in diameter). Overnight, all cells were grown in serum-free DMEM to allow them to synchronize. Cells were given drug treatment for 15 minutes prior to LPS treatment. Lipopolysaccharide (LPS-1000 ng/ml) were applied to cells for the stated times. Cells were then washed with 1X PBS one time after the medium had been aspirated. The cells were fixed for 20 minutes at room temperature with freshly prepared 4% paraformaldehyde and then after washing they were permeabilized for 10 minutes with 0.1% Triton-X 100. Cells were blocked with 5% BSA in 1X Tris-buffered saline, 0.1% Tween®20 Detergent (TBST) for 90 minutes, after fixation and permeabilization, followed by an overnight staining procedure at 4°C using primary antibodies with 1:200 dilution in blocking buffer. The cells were stained with secondary antibodies with dilution 1:500 in 1X TBST for an

hour at room temperature after being washed with 1 TBST three times for 5 minutes each. Nuclear counterstaining along with mounting is carried out in accordance with the manufacturer's instructions using DAPI containing mounting media. The Olympus confocal laser scanning microscope (FV100) was used to study the coverslips after mounting them onto glass slides with mounting fluid. Images were taken at 100X magnifications.

2.1.3. H&E staining

H&E staining is a common histological staining technique used in microscopy to visualize tissue samples. H&E stands for hematoxylin and eosin, which are two dyes used in the staining process.
Hematoxylin is a basic dye that stains the acidic components of cells, such as the nucleus and some cytoplasmic structures, blue to purple. Eosin is an acidic dye that stains the basic components of cells, such as cytoplasm and extracellular matrix, pink to red. Tissue samples preserved in 4% formaldehyde were used for the embedding in paraffin wax, mounting and staining. After viewing the prepared slides under a microscope equipped with an Invitrogen EVOS M5000 Cell Imaging System, images were captured at a magnification of 40X. ImageJ was then used to count the immune cells that had invaded the alveolar space.

2.1.1. Animal studies

Male and female young Swiss albino mice aged 4-5 months were collected from the College of Veterinary Science and Animal Husbandry, Mhow, Indore, Madhya Pradesh, India, in a ratio of 3:2, with each mouse weighing -30g. All mice were kept at a temperature of 25° to 28° C with a 14:10 h light/dark cycle and access to food and water 24 hours a day. Prior to the experiment, mice were housed for seven days. The animal study conducted

was approved by the Institutional Animal Ethics Committee (IAEC) of Acropolis Institute of Pharmaceutical Education and Research and conducted in accordance with the policies of Committee for the Purpose of Control and Supervision of Experiments on Animals (CPCSEA), Govt. of India.

2.1.1. Bacterial Culture

1ml of cecal slurry resuspended in 1X PBS was inoculated in 50 ml Luria Broth (HIMEDIA M575-500G) and was cultured overnight at 37°C on a shaker (220 RPM). The culture was then filtered (70 μm mesh strainer) to remove slurry particles. 1/60th part of that 1° culture (OD=1.5) was then inoculated in 50 ml LB media (2° culture). By utilizing this inoculum volume, the OD reached to 1 after 3 hours of incubation. OD was measured using UV spectrophotometer (PerkinElmer UV/VIS Spectrometer Lambda 35) at 600 nm. Different volumes of the culture media were then used for preparing injections with different bacterial concentration and the remaining media was used for preparing cryovials of 50% glycerol stock which were then stored at −80°C. For enrichment of cultures with a particular type of bacteria, the following specific antibiotics (20 ug/ml) were used: Aztreonam to kill Gram-negative bacteria, and Vancomycin to kill Gram positive bacteria. Antibiotics were added to the secondary culture. To check the growth rate of bacteria in these antibiotics rich media, OD was measured at 600 nm. To validate the growth rate, spreading with primary culture was additionally done on agar plates containing Luria Agar (HIMEDIA M557-500G) and respective antibiotics. These were then observed after overnight incubation at 37°C. Gram staining was performed to confirm the type of microbiota in polymicrobial population. This enrichment culture method was replicated with both fresh cecal slurry and the 2 months stored 50% glycerol stock.

2.1.1. Survival curve analysis

Mice were injected with different polymicrobial concentration and were monitored for up to 48 hours post injection. The Kaplan-Meier curve was used for graphical presentation, where Y-axis represented percent survival. The tissue samples of the lungs, liver and kidneys were collected 10 hours post injection in animals from two groups (2 mice/group). These were preserved in 4% formaldehyde and were analyzed after H&E staining. Each experiment was performed twice, and the survival curve was constructed by the data acquired in each group.

2.1.2. Serum isolation

After 10 hours of anesthesia and subsequently complete death by cervical dislocation, serum was obtained from treated mice. The serum was obtained by puncturing the heart, and the total blood was obtained in 1.5 ml MCT. Serum was obtained as supernatant after centrifugation at 7000 RPM for 25 minutes at 4° C following full coagulation of blood by keeping it at room temperature for 30 minutes, and was then stored in -80°C.

2.1.1. ImageJ analysis

ImageJ allows users to measure various parameters in images, such as intensity, size, shape, and texture. It also provides tools for performing statistical analysis on the image data. Here, it was used to analyze the western blot images, confocal images, and H&E-stained tissue sections images. For western blot images, the band intensity was measured and after normalization with loading control, the intensity of different samples was

compared. For confocal images, the fluorescent intensity was measured after splitting the images into an appropriate channel. For H&E-stained images, the cell number was measured by first splitting the images into an appropriate channel and then setting up of a threshold for appropriate size of cells. The values were then analyzed and plotted in GraphPad PRISM 7.0.4.216 (© 1992-2017 GraphPad Software. lnc).

2.1.2. Gram staining

To validate the enriched culture, whether it is gram positive or negative bacteria, a simple gram staining technique was performed by using gram staining kit (HIMEDIA-K001-1KT), where crystal violet was used to stain gram positive while safranin was used to stain gram-negative bacteria. The culture media was used immediately after measuring the OD.

2.1.1. Statistical analysis

Statistical analysis and visualization of data was performed using GraphPad PRISM 7.0.4.216 (© 1992-2017 GraphPad Software. lnc). All data are representative of two independent experiments; all data are presented as mean $\pm$ SD. P Significance was determined using One-way ANOVA test. **$P \leq 0.01$; *$P \leq 0.01$

3. Chapter 3

3.1. Results and Discussion

3.1.1. TIRAP interacting site with BTK, and PKCδ, -

In gram-negative bacteria, the principal receptor implicated in stimulated signaling is TLR4 stimulated majorly by LPS, which led to activation of NFkB and AP1 transcriptional factors, which led to activation of genes responsible for the release of pro-inflammatory cytokines. TRAF-6, MAPK, and different adaptors such as TIRAP and MyD88 are among the signaling molecules involved in the signaling (Rajpoot et al., 2021b). The most upstream molecule in this signaling is TIRAP, which activates after interacting with and being phosphorylated by BTK and PKC tyrosine kinases, leading to the activation of MyD88. So, TIRAP may interact with BTK, and PKC, and if we can block this interaction, we can entirely block TIRAP-mediated inflammatory signaling. As a result, we were eager to discover TIRAP's interaction site with these two molecules.

TIRAP's interaction sites with BTK and PKC have already been found using molecular docking and MD simulations (Rajpoot et al., 2022).

Interestingly, TIRAP was found to share some common residues while interacting with the two molecules that were P169, F193, M194, Y195 (**Fig. 3.1.1**). Thus, we went for screening the compounds against those residues.
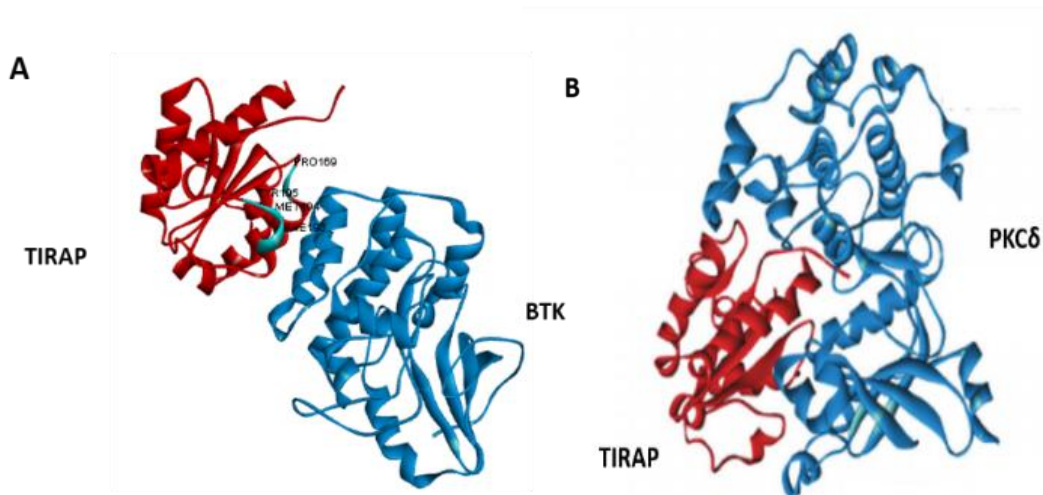
Fig. 3.1.1. Molecular docking structure of BTK-TIRAP, PKCδ-TIRAP, and MyD88-TIRAP (A) Docking structure of TIRAP with BTK, (B) Docking structure of TIRAP with PKCδ.

3.1.2. An FDA approved Repurposed Drug binding to common binding site of TIRAP with BTK, and PKCδ, -

Screening of FDA authorized library against the common binding residues was done in AutoDock Vina and Schrodinger to examine FDA approved library. The best pose with the highest binding affinity was chosen for further investigation. We found a drug with dock score of -6.3 which can be considered as a good binding score which is binding to the desired site (**Fig. 3.2**). We took that drug for further in vitro and in vivo studies.
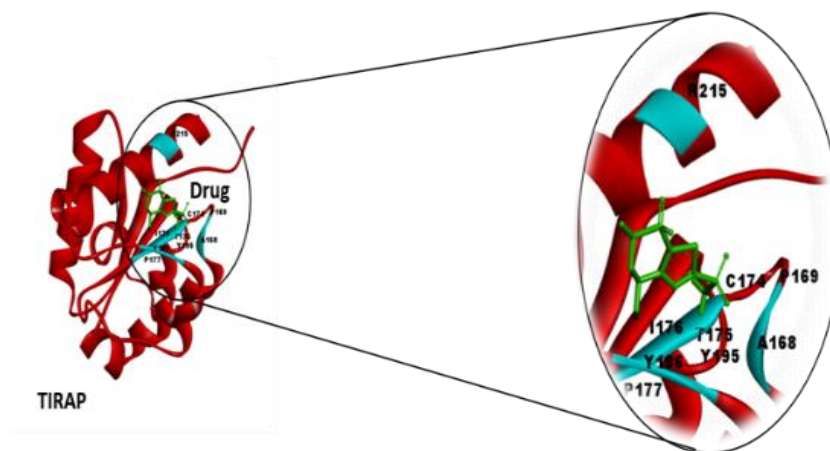
Fig. 3.1.2. Molecular docking structure of TIRAP with the repurposed drug with highlighted interacting residues of TIRAP.

3.1.3. An Antibiotic binding to common binding site of TIRAP with BTK, and PKCδ -

FDA-approved docking in the AutoDock Vina and Schrodinger software was utilized to screen antibiotic binding to the TIRAP interaction region. The best pose was chosen for further investigation, and one antibiotic with a dock score of -7.7 was discovered to bind more efficiently and was chosen for in vitro and in vivo research (**Fig. 3.1.3**).
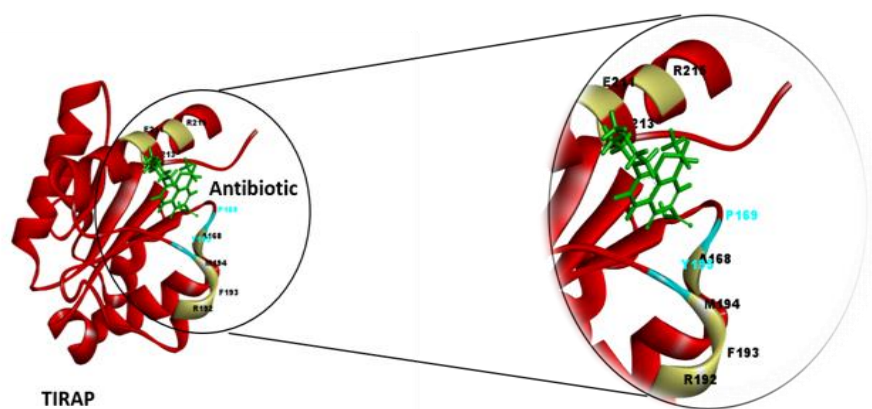
Fig. 3.1.3. Molecular docking structure of TIRAP with the screened antibiotic with highlighted interacting residues.

19

3.1.4. Repurposed Drug show anti-inflammatory effects in vitro-

TIRAP activation by phosphorylation resulted in the induction of the transcriptional factors NFkB and AP1 via p38 MAPK. NFkB is activated by phosphorylation at its p65 subunit at ser 536 amino acid, which is then detached from the p50 subunit and translocated to the nucleus, where it activates the genes involved for the expression of pro-inflammatory cytokines such as IL-1b and TNF-a. Similarly, phosphorylation activates the c-Jun component of the AP1 transcriptional factor, causing it to translocate to the nucleus and activate the genes responsible for the release of pro-inflammatory cytokines such as IL-12 and IL-23. And phosphorylation activates p38, which can activate both of these transcription factors. If the RD can suppress the activation of these proteins, we might claim that the drug is operating as an anti-inflammatory drug. Thus, we sought for the activation of these protein molecules, and for the mechanistic viewpoint, we looked for the activation of TIRAP, which is activated by phosphorylation by tyrosine kinases like BTK and PKCδ.

3.1.4.1. RD downregulates NFkB activation

When NFkB's two subunits, p65 and p50, are bound to one another, they are inactive but become active and translocate to the nucleus when the p65 subunit is separated from its binding partner. Kinases can either directly phosphorylate the p65 subunit and unbind it from the p50 subunit, or they can activate the enzymes responsible for degrading the protein molecule IκBα or IκBβ, which aids in the binding of these subunits. As a result, the phosphorylation of the p65 subunit can be examined to determine the anti-inflammatory activity of the NFkB transcriptional factor.

To see if the drug inhibits NFkB signaling in LPS-stimulated macrophages, we treated RAW 264.7 cells with RD and then stimulated them with LPS. The immunoblot data showed that LPS activated macrophages for 1 hour

had much reduced phosphorylation in the presence of the drug (**Fig. 3.1.4.1.1**.). According to the immunofluorescence results, p65 is less translocated in the nucleus of one-hour LPS stimulated macrophage cells treated with the drug (**Fig. 3.1.4.1.2**.). This information indicates that the drug inhibits NFkB-mediated inflammatory signaling.
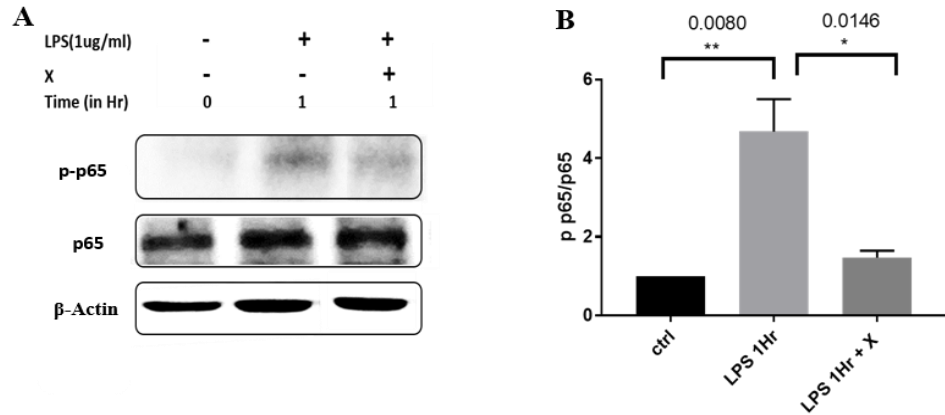
Fig. 3.1.4.1.1.: The effect of RD (X) on LPS-stimulated TLR4 signaling in RAW 264.7 cells. (A-B) Immunoblot analysis of p65 indicates significant downregulation of p65 phosphorylation. All experiments were independently performed for three times.
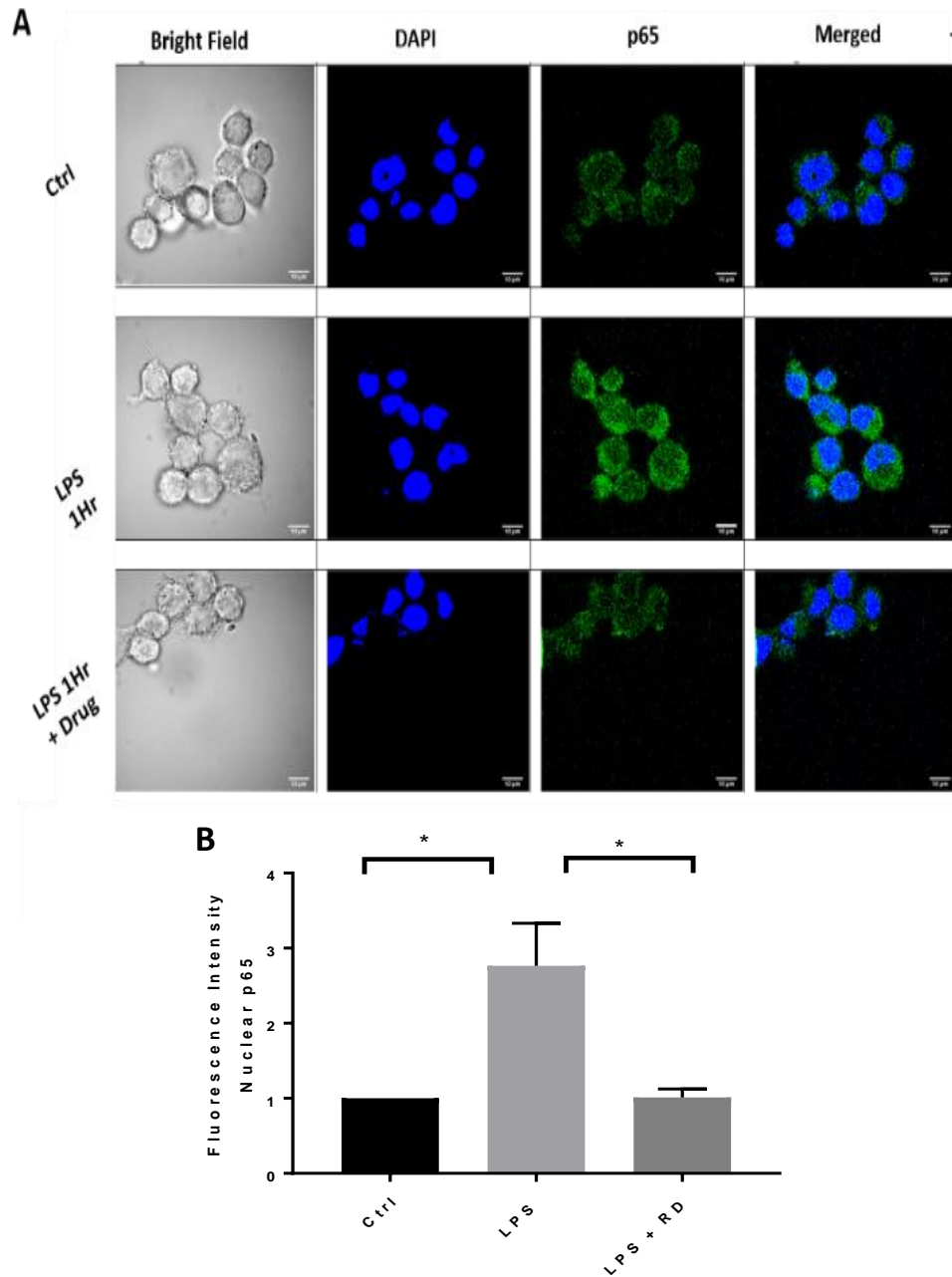
Fig. 3.1.4.1.2.: The effect of RD on LPS-stimulated (1ug/ml) TLR4 signaling in RAW 264.7 cells. (A-B) Immunofluorescence data indicating inhibition of nuclear translocation of NF-kB p65 in X treated cells. All experiments were independently performed for three times.

3.1.4.2.RD downregulates NFkB and AP1 signaling via p38 activation-

TIRAP regulates AP1 and NFkB activation via a single p38 MAPK, which becomes active upon serine phosphorylation and upregulates both transcriptional factors.

To assess p38 activation in LPS-stimulated macrophages treated with RD, we performed immunoblot analysis, which revealed lower p38 activation in drug-treated macrophages (**Fig. 3.1.4.2**). This suggests that the medication is suppressing something that is upstream of both transcription factors and p38 MAPK.
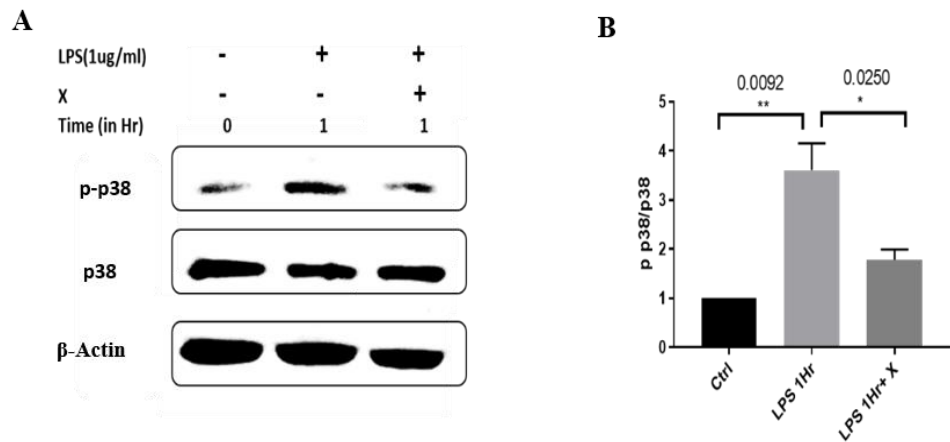
Fig. 3.1.4.2: The effect of RD (X) on LPS-stimulated TLR4 signaling in RAW 264.7 cells. (A-B) Immunoblot analysis of MAPK p38 indicates significant downregulation of MAPK p38 phosphorylation. All experiments were independently performed for three times.

3.1.4.3.RD downregulates AP1 mediated proinflammatory cytokines-

The expression level of mRNA of AP1 regulated pro-inflammatory cytokines in RD treated and LPS stimulated macrophages was compared using RT-PCR to further confirm the downregulation of AP1 transcriptional factor by the RD. Among these AP1-regulated pro-inflammatory cytokines, IL-12 and IL-23 mRNA expression levels were observed to be considerably reduced when LPS-stimulated macrophages were treated with the RD (**Fig. 3.1.4.3**.). The total RNA was isolated and 1ug from each sample was used for single stranded cDNA preparation as per manufacturer instruction. The prepared cDNA was used as template for real time PCR and relative mRNA expression of pro-inflammatory cytokines were estimated with respect to GAPDH.
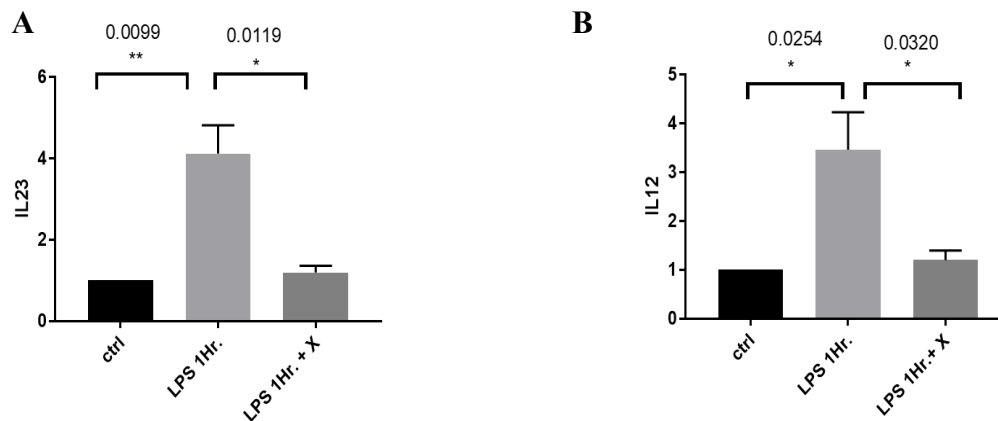
Fig. 3.1.4.3: Effect of RD (X) on AP1 mediated pro-inflammatory cytokines mRNA expression in LPS-induced RAW 264.7 cells. (A) Relative mRNA expression of IL-23 in RAW 264.7 cells (B) Relative mRNA expression of IL-12 in RAW 264.7 cells. Both experiments were independently performed for three times.

3.1.4.4.RD downregulates TIRAP activation-

The data in sections 3.4.1-3.4.3 demonstrated that RD suppressed the inflammatory response. So, we looked for the most upstream and computationally proven target TIRAP, which likewise gets activated after tyrosine phosphorylation at particular amino acid residues, such as Tyrosine at the 86th position of the polypeptide chain of TIRAP's TIR domain. Tyrosine kinases such as BTK phosphorylate membrane-bound TIRAP and PKC**δ** phosphorylate cytoplasmic TIRAP.

To assess TIRAP activation, LPS-stimulated macrophages were treated with RD, and immunoblot analysis revealed that the drug-treated cells had less phosphorylated TIRAP than the LPS-stimulated cells (**Fig. 3.1.4.4**). This highlights that the computationally screened drug is inhibiting the same target with high efficiency. Therefore, from invitro studies we are confirmed that the drug is acting as an anti-inflammatory drug.
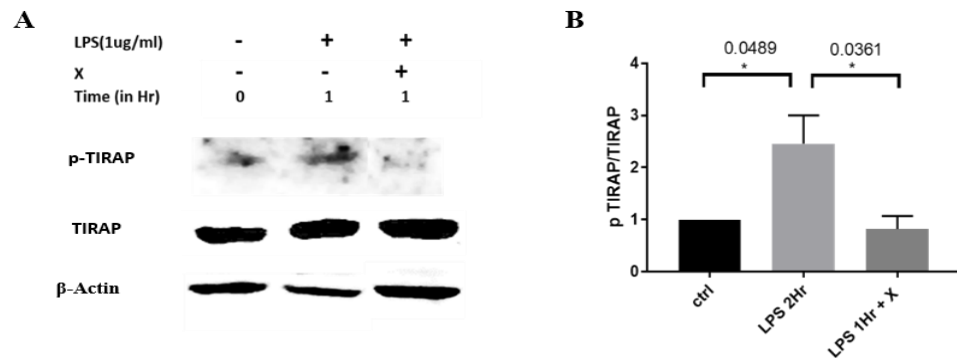
Fig. 3.1.4.4: The effect of RD (X) on LPS-stimulated TLR4 signaling in RAW 264.7 cells. (A-B) Immunoblot analysis of TIRAP indicates significant downregulation of TIRAP phosphorylation. All experiments were independently performed for three times.

3.1.5. RD show anti-inflammatory effects in vivo-

Sepsis mostly affects the lungs, liver, and kidneys, which begin to deteriorate after a persistent inflammatory illness. This begins when a pathogen infects any of these organs, and then the stimulants or pro-inflammatory cytokines released in response to that stimulant at the infected location travel to other organs via the bloodstream, where they commence the inflammatory response. As a result, when the inflammation in those tissues becomes dysregulated and a chronic-inflammatory disease develops, it leads to multi-organ damage known as severe sepsis. So, we can measure the survival of mice, the inflammatory condition in the lungs tissue because this is the organ that is damaged, and the level of pro-inflammatory cytokines in the serum to check if the drug has an anti-inflammatory impact. To see the in vivo effect of the drug Swiss albino mice were used in which sepsis was induced by intraperitoneal injection of LPS.

3.1.5.1.RD increase the survival rate in LPS infected mice-

To see the effect of the drug on the survival of mice, four groups of 12 mice each with male and female mice in the ratio of 3:2 were prepared. One group was kept as control, second was injected with LPS intraperitoneally as positive control, third with only RD intravenously as negative control, and fourth with LPS and RD one hour prior to LPS injection. Then, the survival was observed till 78 hours.

From the experiment, we observed that there was about total 70% mortality in the only LPS treated group and only 40% mortality in the LPS treated group along with the drug (**Fig. 3.1.5.1**). There was no death in only drug treated group telling non-toxicity of the drug. So, the RD increased the survival by 30% which is also giving the information of the role of inflammation in the progression of sepsis.
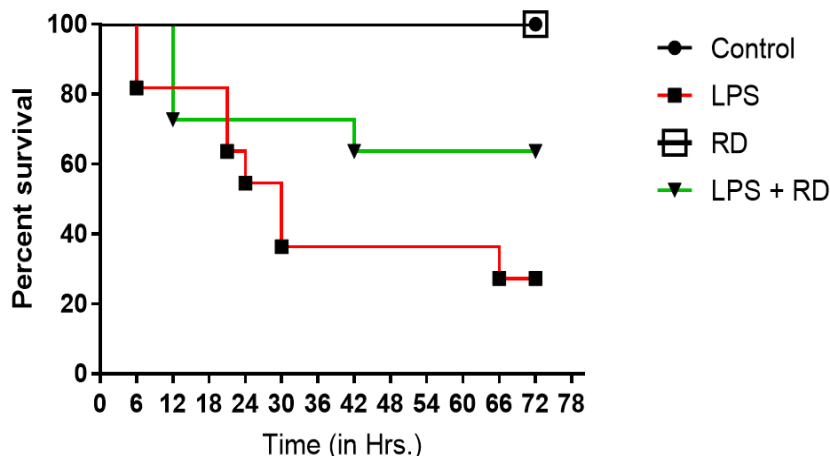
Fig. 3.1.5.1: Survival curve of mice treated with RD for 78 hours.

3.1.5.2.RD decrease the infiltration of immune cells in alveolar septum-

Lungs are the first and the major organs which get damaged during the sepsis progression. When any pathogen or the endotoxin invade there, the immune cells start infiltrating in the alveolar septum and cause inflammation there and when it persists for a long time the phagocytic immune cells start engulfing the lungs cells leading to necrosis and tissue damage.

To determine the immune cells infiltration and the necrosis, we collect the lung tissue from every group and perform H&E staining after sectioning and mounting. When the H&E-stained tissue sections were observed under microscope at 10X, 20X, and 40X, the decreased immune cells infiltration in the LPS with RD treated group could be clearly seen (**Fig. 3.1.5.2A**). The necrosis can also be observed by the disrupted alveolar septum from 40X

27

image in the LPS treated group which was not observed in the LPS and the drug treated group (**Fig. 3.1.5.2A**). The number of infiltrating immune cells were also calculated by considering 40X images by using ImageJ software. There we could clearly see that the number was decreased in the drug treated septic group (**Fig. 3.1.5.2B**). Therefore, the drug is successful in producing an anti-inflammatory effect.
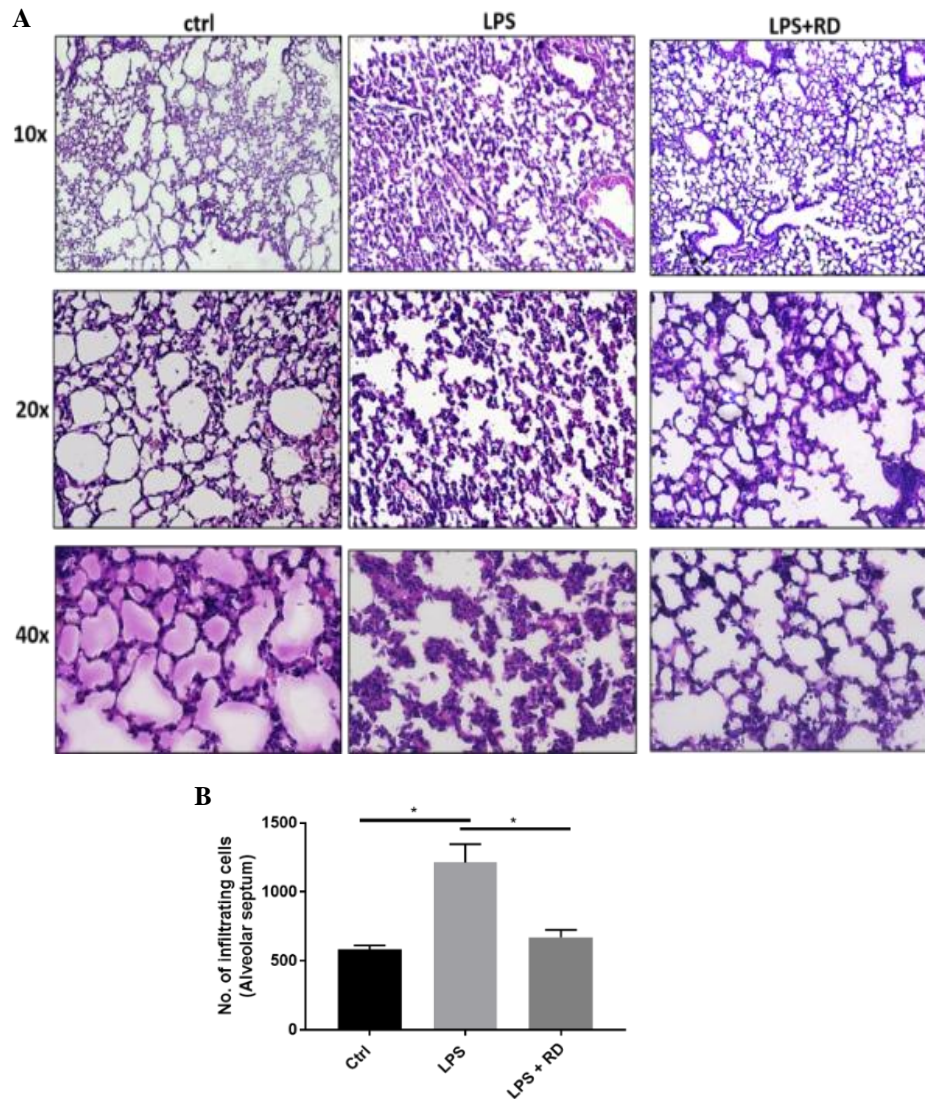
Fig. 3.1.5.2: Lungs tissue sections images for observing the inflammation in the alveolar septum. (A) Lungs tissue images at 10X, 20X, and 40X of three mice groups- control, LPS, and RD treated septic mice group. (B) number of infiltrating immune cells in the alveolar septum considering 40X images. The experiments were conducted three times independently.

3.1.5.3.RD decrease the pro-inflammatory serum cytokines level-

The anti-inflammatory effect of the drug was proved by the lungs tissue sections. To further validate at cytokines level, the blood from the heart of the mice was collected after puncturing. After which serum was isolated and was stored or used for cytokines analysis. And the cytokines level was measured by using cytokines ELISA kit. The major pro-inflammatory cytokines that can led to the diseased condition are TNF-a and IL-1b.

To determine the level of these pro-inflammatory cytokines in the serum of the treated mice, the serum from three mice groups- control, LPS induced septic group, and RD treated septic mice group, was isolated and level of cytokines was analyzed. From the data, we observed that the both the pro-inflammatory cytokines were in less amount when the LPS induced septic mice were treated with the RD (**Fig. 3.1.5.3**). Therefore, this data made us sure that the drug has significant anti-inflammatory action.
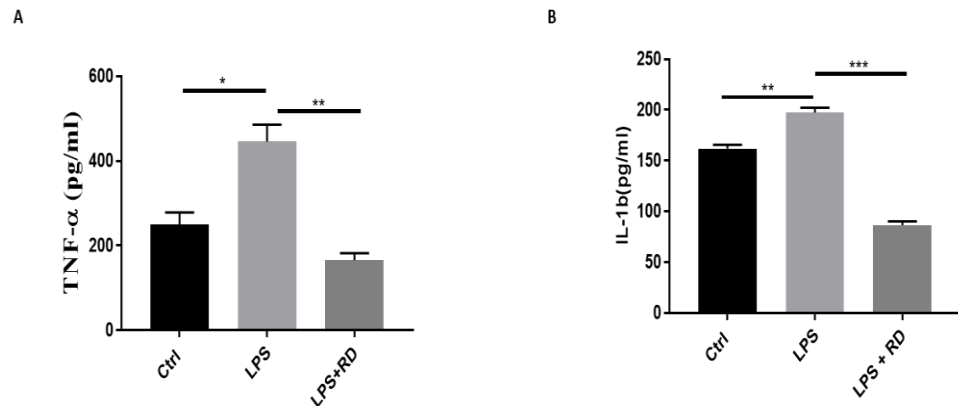
Fig. 3.1.5.3: Serum cytokine level in pg/ml analyzed with cytokines ELISA kit. (A) TNF-a level was significantly decreased when the septic mice group (B) IL-1b level was significantly decreased when the septic mice group. The experiment was replicated three times independently.

3.1.6. Antibiotic show anti-inflammatory effects-

TIRAP activation by phosphorylation resulted in the induction of the transcriptional factors NFkB and AP1 via p38 MAPK. NFkB is activated by phosphorylation at its p65 subunit, which is then dissociated from the p50 subunit and translocated to the nucleus, where it activates the genes involved for the release of pro-inflammatory cytokines such as IL-1b and TNF-a. Similarly, phosphorylation activates the c-Jun component of the AP1 transcriptional factor, causing it to translocate to the nucleus and activate the genes responsible for the release of pro-inflammatory cytokines such as IL-12 and IL-23. And phosphorylation activates p38, which can activate both the transcription factors.

So, if the antibiotic, like RD, can suppress the activation of these proteins, we may conclude that the antibiotic is operating as an anti-inflammatory chemical. So, we looked for the activation of these protein molecules, and for the mechanistic viewpoint, we looked for the activation of TIRAP.

3.1.6.1.Ab downregulates NfkB activation-

NFkB has two subunits, p65 and p50, which are bound to one another, they are inactive but become active and translocate to the nucleus when the p65 subunit is liberated from its binding partner. Kinases can either directly phosphorylate the p65 subunit and unbind it from the p50 subunit, or they can activate the enzymes responsible for degrading the protein molecule IKK, which aids in the binding of these subunits. As a result, the phosphorylation of the p65 subunit can be examined to determine the anti-inflammatory activity of the antibiotic against the NFkB transcriptional factor.

To see if the antibiotic inhibits NFkB signaling in LPS-stimulated macrophages, we treated RAW 264.7 cells with antibiotic and then stimulated them with LPS. The immunoblot data showed that LPS

stimulated macrophages for 1 hour had much reduced phosphorylation in the presence of the antibiotic (**Fig. 3.1.6.1**.).

A   **B**
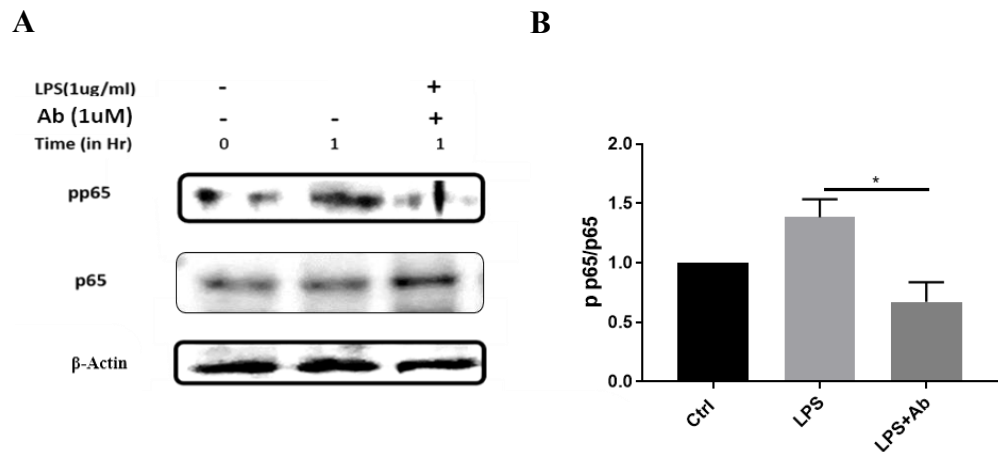
Fig. 3.1.6.1: The effect of antibiotic (Ab) on LPS-stimulated TLR4 signalling in RAW 264.7 cells. (A-B) Immunoblot analysis of p65 indicates significant downregulation of p65 phosphorylation. All experiments were independently performed for three times.


3.1.6.2.Ab downregulates AP1 activation-

TIRAP regulates AP1 and NFkB activation via a single p38 MAPK, which becomes active upon serine phosphorylation and upregulates both transcriptional factors.

To assess p38 activation in LPS-stimulated macrophages treated with antibiotic, we used immunoblot analysis, which revealed lower p38 activation in antibiotic-treated macrophages (**Fig. 3.1.6.2**). This suggests that the medication is suppressing something that is downstream of both transcription factors and p38 MAPK.
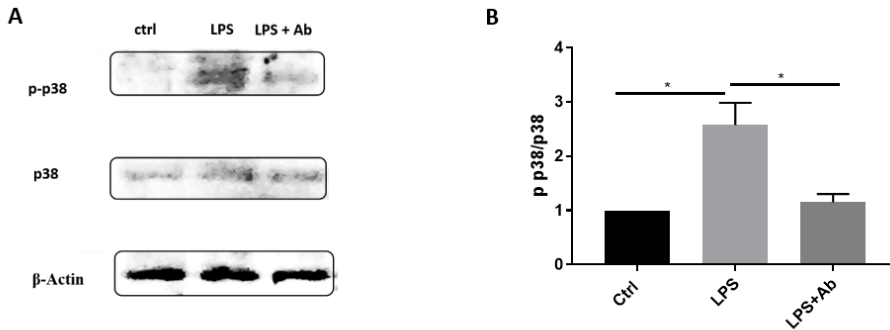
Fig. 3.1.6.2: The effect of antibiotic (Ab) on LPS-stimulated TLR4 signaling in RAW 264.7 cells. (A-B) Immunoblot analysis of MAPK p38 indicates significant downregulation of MAPK p38 phosphorylation. All experiments were independently performed for three times.

3.1.6.3.Ab downregulates TIRAP activation-

The data in sections 3.6.1 and 3.6.2 demonstrated that RD suppressed the inflammatory response. So, we looked for the most upstream and computationally proven target TIRAP, which likewise gets activated after tyrosine phosphorylation at particular amino acid residues. Tyrosine kinases such as BTK phosphorylate membrane-bound TIRAP and PKCd phosphorylate cytoplasmic TIRAP.

To assess TIRAP activation, LPS-stimulated macrophages were treated with antibiotic, and immunoblot analysis revealed that the antibiotic-treated cells had less phosphorylated TIRAP than the LPS-stimulated cells alone (**Fig. 3.1.6.3**). This demonstrates that the computationally screened antibiotic effectively inhibits the same target. As a result of the in vitro experiments, we may conclude that the antibiotic acts as an anti-inflammatory agent.
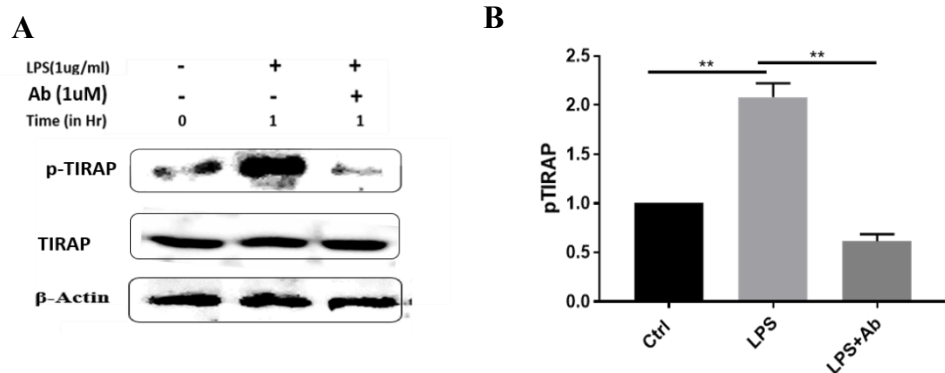
Fig. 3.1.6.3: The effect of antibiotic (Ab) on LPS-stimulated TLR4 signaling in RAW 264.7 cells. (A-B) Immunoblot analysis of TIRAP indicates significant downregulation of TIRAP phosphorylation. All experiments were independently performed for three times.

3.1.7. Development of septic mouse model-

Animal sepsis models are widely used to study the pathophysiology of sepsis. However, it is crucial to identify the right model which can be reproducible and capable of mirroring both cellular and molecular aspects of sepsis, such as observed in humans. Several approaches have been developed in the past to study sepsis. These include the CLP (Share, 1976a) , CASP (Gardos & Cole, 1976), CS (Parry et al., 1976b) methods and few others. The CLP approach is considered as the "Gold standard" to develop and replicate the human condition of polymicrobial infection in animals (Share, 1976b). Despite its wide acceptance, it has several shortcomings. This model is complicated due to high variability in

terms of size and shape of cecum that ultimately affects sepsis severity. Similarly, such models as CASP (Dorofeyeva, 1975) and CS (Parry et al., 1976c) that are also aimed to mirror sepsis conditions recapitulating the human state have limitations. These models require the sacrifice of

33

additional animals for every single new experiment. Furthermore, these approaches do not provide a sufficient insight on the microbial flora composition that is delivered into the abdominal cavity from the cecum, bringing the uncertainty factor in the induction of sepsis

model. In the CS model, the slurry is prepared fresh every time, thus adding a high amount of variability every time the experiment is performed. Though a new method was recently developed where storage option has been proposed, making an alternative to animal sacrifice for each experiment, the approach still lacks the reproducibility of sepsis conditions among different experiments and again lacks information on the composition of microbial population. Hence, a better and improved approach is required to tackle the obstacles being faced in the development of sepsis models. Herein we propose a novel and efficient method for inducing polymicrobial sepsis in animals. Our protocol is based on the intraperitoneal injections of defined bacterial cultures with known polymicrobial population. In our experiments, we compared five animal groups, including a control group. Each treatment group received varying doses of polymicrobial bacterial load. Before animal injection, the polymicrobial cultures were grown in the standard LB medium that is a standardizable approach, allowing sepsis induction with varied titrated inoculum dosages in order to develop the diseased state with varying severity as per the requirement. The results from the survival curves depict that the groups injected with higher CFU had early mortality and the mortality rate decreased with the decreases in CFU. This can prove to be helpful in order to regulate and plan the experiments to better understand the biology and various factors involved at varying stages of sepsis.

3.1.7.1. Development of polymicrobial septic model-

The current study describes the creation of an improved approach for inducing sepsis that is reproducible and standardised. Our innovative

method is based on intraperitoneal injection of a known amount of enriched polymicrobial population obtained from cecum slurry and propagated in LB media until a desired bacterial density, as determined by optical density (OD), is reached. In this paper, we propose storing cultivated poly microbiota in glycerol stocks at 80°C to maintain a consistent bacterial population throughout numerous tests. The new technique has an ethical edge over prior methods since it eliminates the need for gratuitous animal sacrifice while making the cecum slurry for each experiment. (Atre et al., 2023).

3.1.7.1.1. Effect of different bacterial concentrations on survival of mice –

To investigate the influence of bacterial concentrations on the mortality of mice with experimental sepsis, we divided 44 mice into five groups (A, B, C, D, and E), with each group including 8-10 mice (two extra mice in groups C and D for tissue collection). The mice were injected intraperitoneally with either 2x10 9 CFU/ml (group A), 1x10 9 CFU/ml (group B), 0.5x10 9 CFU/ml (group C), or 0.1x10 9 CFU/ml (group D) bacterial suspension, while group E served as a control (**Fig. 3.1.7.1.1**). We employed a bacterial culture with an optical density of 1OD (measured at 600 nm) and transferred 2 ml, 1 ml, 0.5 ml, and 0.1 ml into four sterile individual centrifuge tubes to produce the aforementioned bacterial concentrations. An 1OD bacterial culture has been reported to have a bacterial concentration of roughly 10 9 CFU in 1 ml of culture media. Following centrifugation, each pellet was dissolved in 500 l 1X PBS and intraperitoneally injected into each mouse. Mice were checked every 2 hours. We observed 80% death in group A after 6 hours, 50% mortality in group B after 6 hours, 50% mortality in group C after 16 hours, and only 20% mortality in group D after 20 hoursWith the highest bacterial

concentration after 16 hours post injection, group A experienced 100% mortality. In contrast, only 20% of the mice in group D with the lowest concentration died after 20 hours, and all survivors recovered quickly **(Fig. 3.1.7.1.1).** When examined closely, all mice in groups A, B, and C suffered white eyes and loss of eyesight after 12 hours, indicating severe sepsis. The mouse eyes in group D remained unaltered, indicating that there was insufficient polymicrobial concentration to trigger severe sepsis. To validate the results, the entire experiment was duplicated using the polymicrobial cultures' glycerol stock. To validate the results, the entire experiment was duplicated using the polymicrobial cultures' glycerol stock.
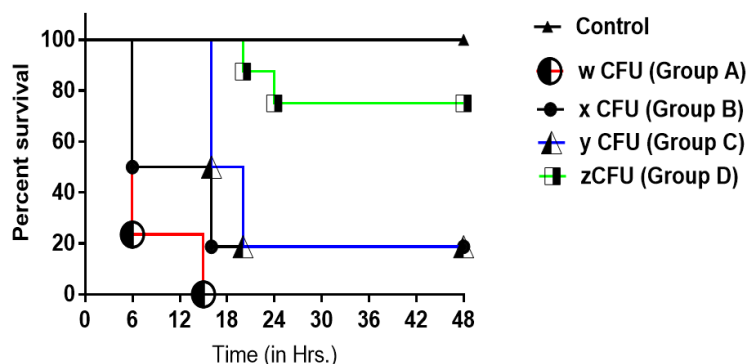
Fig. 3.1.7.1.1: The survival curve in mice treated with $2X10^9$ CFU/ml (w), $1X10^9$ CFU/ml (x), $0.5X10^9$ CFU/ml (y), and $0.1X10^9$ CFU/ml (z) (8 mice per group).

3.1.7.1.2. Effect of different bacterial concentration on different organs of mice-

The group C lung tissue consistently had more infiltrating immune cells than the group D lung tissue. Using ImageJ packed with 64-bit Java 8 and 536x389 pixels images, we additionally evaluated the number of cells invading the alveolar septum (Fig. 3.1.7.1.2B) and the unoccupied space between the septum (Fig. 3.1.7.1.2E). We discovered that the degree of

immune cell infiltration corresponded well with the polymicrobial concentration, and that the unoccupied space decreased in accordance with it, plainly demonstrating that sepsis became more severe as inflammation increased. The alveoli were more damaged in group C than in group D, indicating that the severity of sepsis increased in group C. The liver tissue was then compared **(Fig. 3.1.7.1. 2A).** We identified more immune cells and higher necrosis affected areas in group C than in group D, showing that high polymicrobial concentrations increased inflammation and tissue damage. A similar trend was observed in the kidneys **(Fig. 3.1.7.1. 2A).** We also counted the number of invading immune cells and the % of necrotic region in the liver **(Fig. 3.1.7.1. 2C and 2F)** and kidney **(Fig. 3.1.7.1. 2D and 2G),** and both increased. In brief, all three organs had elevated inflammation and showed evidence of multi-organ damage, which likely proceeded to sepsis and ultimately septic shock, which resulted in animal death.
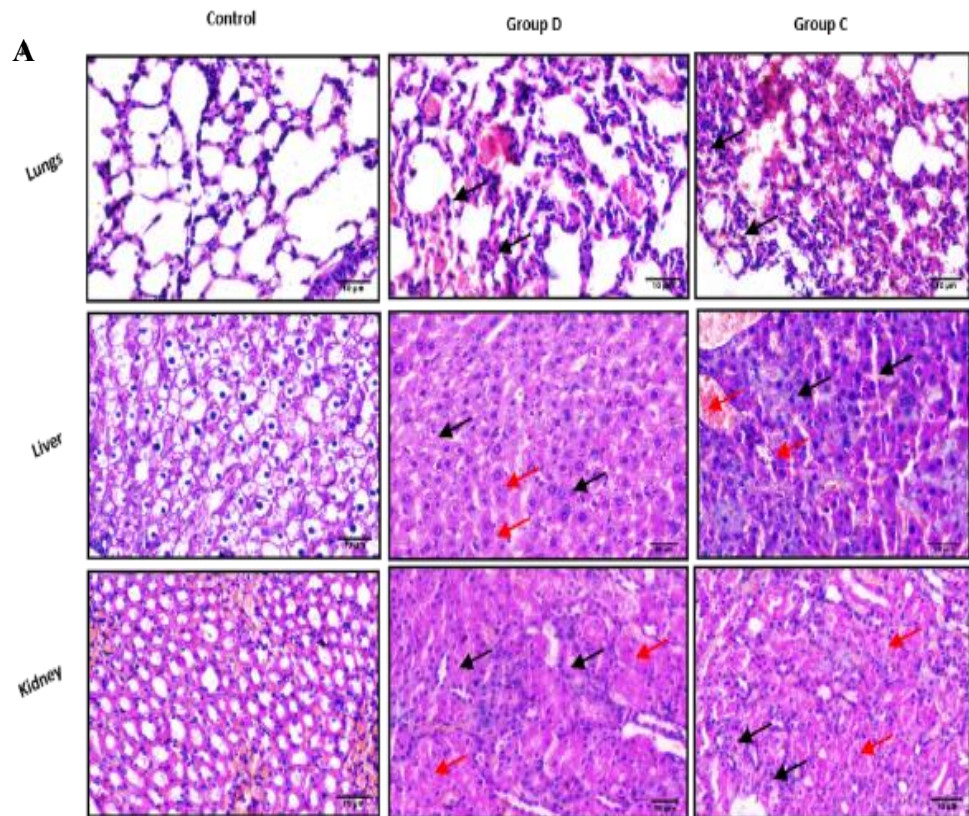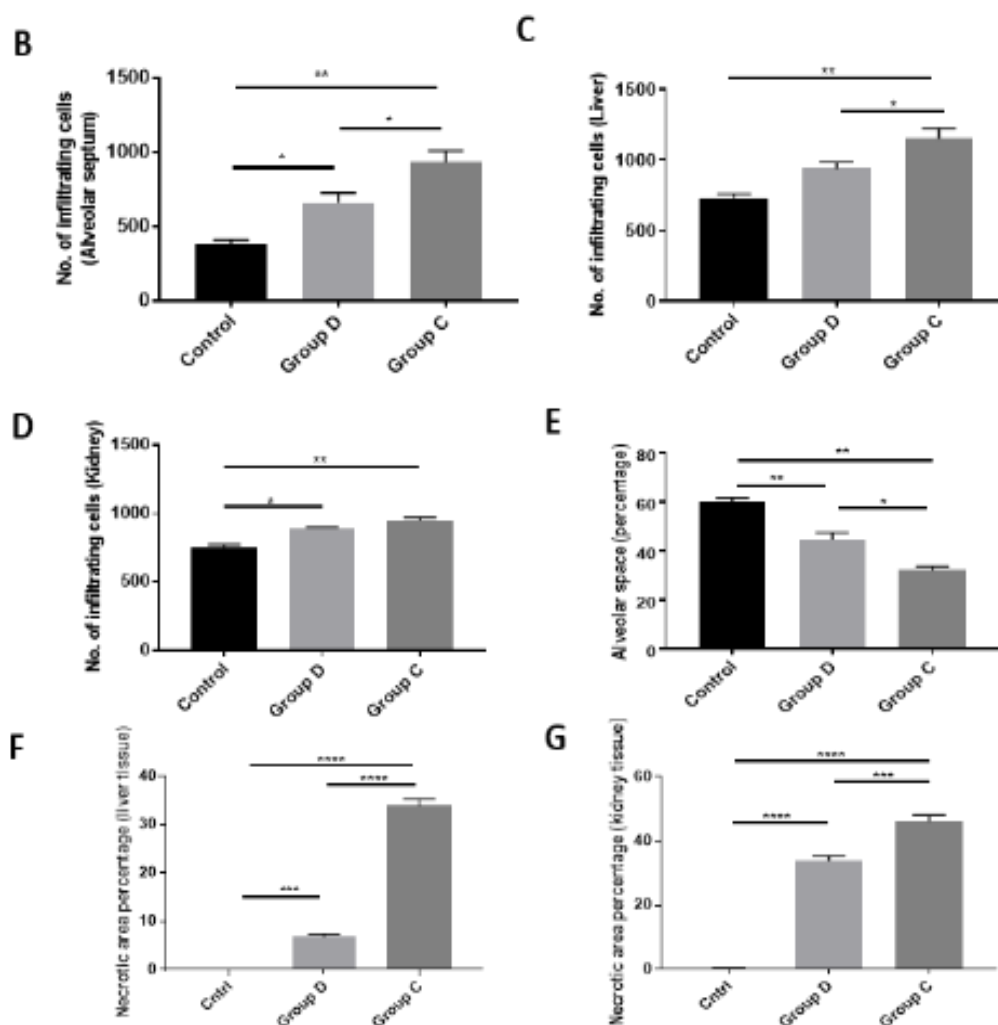
Fig. 3.1.7.1.2: The effect of polymicrobial concentration in cecal slurry on mice. (A) H&E-stained lung, liver, and kidney tissue sections at 40X (10 μm scale bars). The samples were obtained from mice that had not been treated, as well as animals that had been treated with polymicrobial cultures at concentrations of 0.5X10 9 CFU/ml and 0.1X10 9 CFU/ml (black arrow and red arrow represent immune cell infiltration and necrotic region, respectively). The numbers of immune cells entering the alveolar septum, liver, and kidney are depicted in (B)-(D). The proportion of alveolar gap between the alveolar septum is displayed in (E). (F)-(G) represent the proportion of necrotic region in the liver and kidney, respectively. The entire experiment was repeated with a polymicrobial culture

stock of 50% glycerol. All data are representative of two independent experiments; all data are presented as mean ± SD. P Significance was determined using One-way ANOVA test. **P ≤ 0.01; *P ≤ 0.01.

3.1.7.2. Development of gram-negative or gram-positive bacteria induced septic model-

The procedures described above were carried out in order to create polymicrobial sepsis. We again repeated the procedure, but this time we employed enhanced bacterial cultures to produce gram-negative or gram-positive bacterial sepsis. We used two antibiotics, aztreonam and vancomycin, which can target either gram-negative or gram-positive bacteria. In addition, we administered levofloxacin, a broad-spectrum antibiotic, to see if there was any growth other than bacteria. In each of five 15 ml tubes, we added 5 ml LB media and supplemented the media with the appropriate antibiotics (20g/ml), then labelled the tubes as follows: tube A (Blank), tube B (LB + Inoculum), tube C (LB + Aztreonam + Inoculum), tube D (LB + Vancomycin + Inoculum), and tube E (LB + Levofloxacin + Inoculum). The antibiotic-containing media was injected with 1:50 part primary culture (1.5 OD) and incubated at 37 °C for 3 hours on a shaker at a rate of 220 rotations per minute. The tubes were then placed on ice, and the OD was measured at 600 nm with a UV spectrophotometer to determine the growth pattern of bacteria under various conditions. The OD of culture media containing no antibiotics was 0.75, whereas Aztreonam, vancomycin, and levofloxacin enriched cultures had values of 0.41, 0.7, and 0.05, respectively (**Fig. 3.1.7.2A**), indicating that the broad-spectrum antibiotic levofloxacin can kill all types of bacteria and that no fungi were present in the cecal slurry. Notably, gram-positive bacteria developed more slowly than gram-negative bacteria. We also disseminated polymicrobial cultures on agar plates with no antibiotics (**Fig. 3.1.7.2C-a**), aztreonam (**Fig. 3.1.7.2C-b**), vancomycin (**Fig. 3.1.7.2C-c**), or levofloxacin (**Fig. 3.1.7.2C-d**) for additional validation. The results revealed the same trend of increase as measured by OD

values at 600 nm. We next did gramme staining to check the effect of the antibiotics by extracting 20 µl of suspension from each tube and creating smears on slides. We used the HIMEDIA-K001-1KT kit for gram-staining and examined the stained smears under a 40X microscope. There was proliferation of all types of bacteria in cecal slurry, which can be shown using violet and pink stains (**Fig. 3.1.7.2B-a**). More gram-positive bacilli bacteria were identified by crystal violet in tube C, and strings of gram-positive bacilli, which cannot be formed by gram-negative bacilli, were also observed. Accordingly, more gram-negative cocci and bacilli were found in Tube D **(Fig. 3.1.7.2B-c).** There was no growth of any microbial community in Tube E, as expected (**Fig. 3.1.7.2B-d**). The enriched culture can be maintained at 80°C as 50% glycerol stocks for future investigations, or it can be used to induce gram-negative or gram-positive sepsis in mice by using the corresponding cultures at 1 OD and injecting the mice with the required bacterial concentrations. Furthermore, the cultures can be propagated to increase the size of a specific bacterial population.
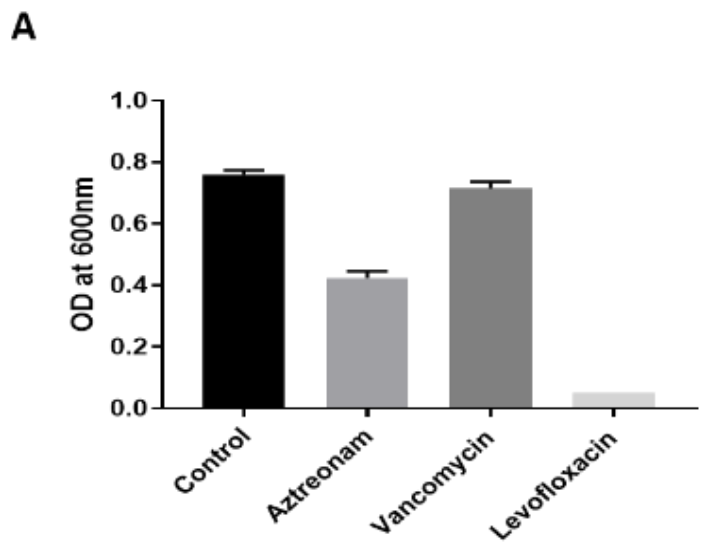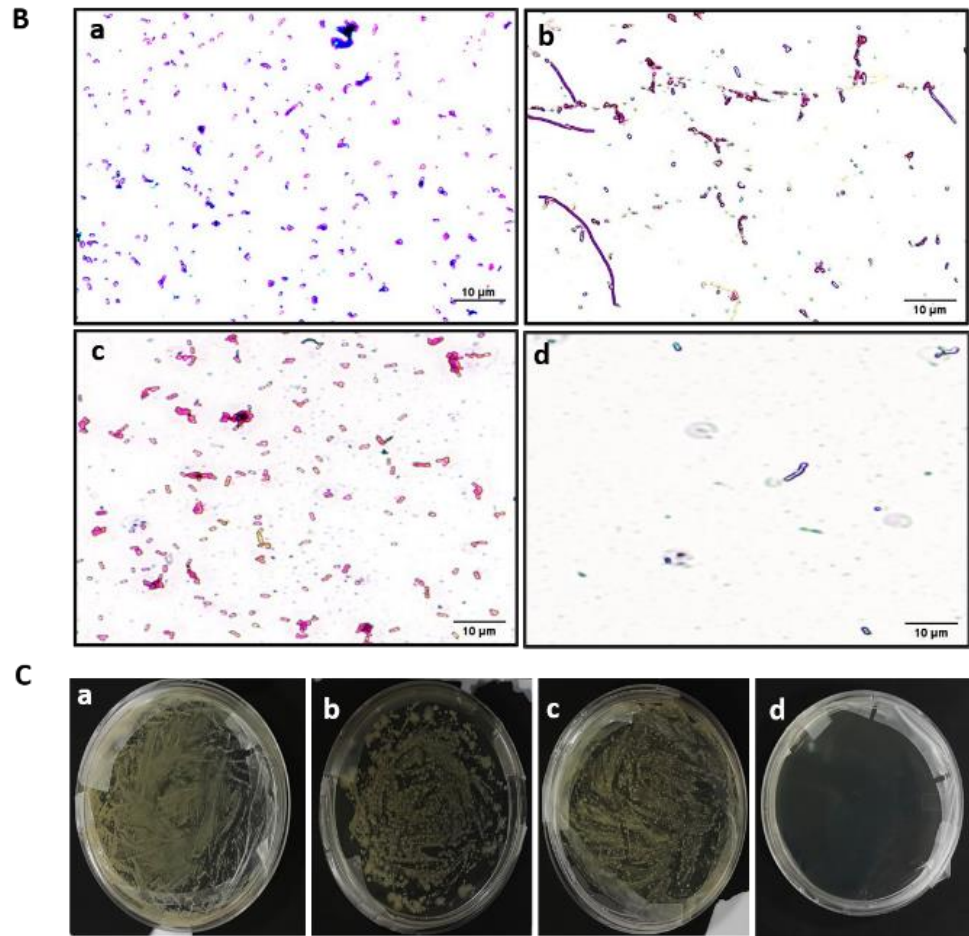
Fig. 3.1.7.2: Culturing cecal slurry poly microbiota in media enriched with antibiotics (20 ug/ml) targeting gram –ve and +ve bacteria. (A) The bar graph depicts the growth rate of bacteria under different conditions, where Aztreonam, vancomycin, and levofloxacin targets gram –ve bacteria, gram +ve and both, respectively. Levofloxacin was used to determine whether there are any other microbes beside bacteria in the cecal slurry. The OD was taken after 3 hours and the error bar shows the OD value after 3.30 hours. (B) The gram-stained images at 40X, where (a) the culture without antibiotics, (b) aztreonam treated culture, (c) vancomycin treated culture, and (d) levofloxacin treated culture. (C) The growth patterns with different antibiotics. LB culture media was spread on LA with (a) no antibiotics (b) aztreonam (c) vancomycin (d) levofloxacin.

41

3.1.8. Synergistic anti-inflammatory effect of antibiotic and repurposed drug in vitro-

To see the combined effect of antibiotic and the repurposed drug, the activation of NFkB, AP1, and p38 was observed. Similar to NFkB which is activated after phosphorylation of p65 and the later then translocate to the nucleus to upregulate the expression of pro-inflammatory cytokines, AP1 is also activated after phosphorylation of c-Jun which is also a subunit of AP1 transcriptional factor and then the phosphorylated c-Jun get translocated to the nucleus to regulate the expression of pro-inflammatory cytokines.

3.1.8.1.Downregulation of NFkB activation-

To determine the combined synergistic effect of the RD and the antibiotic on the activation of NFkB transcriptional factor, the LPS stimulated macrophages were treated with antibiotic, repurposed drug, and the combined drugs. The phosphorylation of p65 was then analyzed by immunoblotting and the phosphorylation was observed significantly less in combined drug treated macrophages comparing to the individual drug treated cells (**Fig. 3.1.8.1**). This highlights the significant synergistic effect when the antibiotic and the repurposed drug are combined.
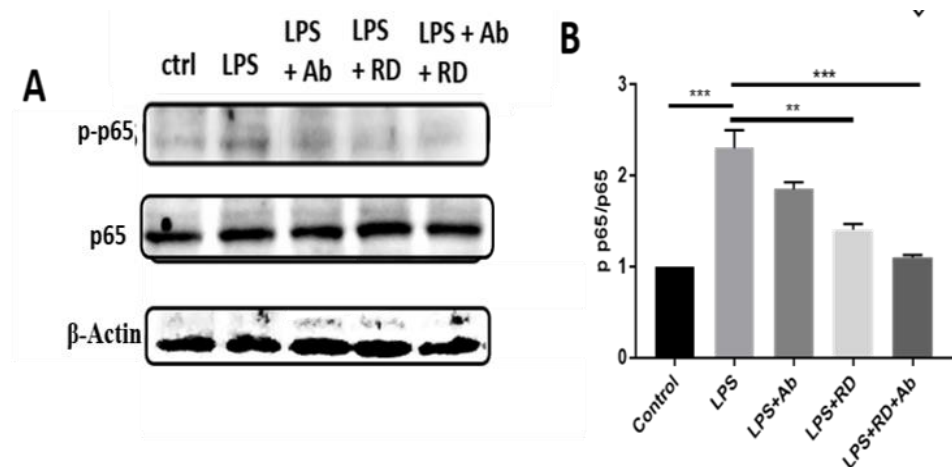
Fig. 3.1.8.1: The combined synergistic effect of the antibiotic and the repurposed drug. (A-B) Immunoblot analysis for phospho-p65 showing significant decrease in the both drugs treated cells. The experiment was replicated three times individually.

3.1.8.2.Downregulation of AP1 transcriptional factor-

Phosphorylation activates the c-Jun component of the AP1 transcriptional factor, causing it to translocate to the nucleus and activate the genes responsible for the release of pro-inflammatory cytokines such as IL-12 and IL-23.

Like NFkB, the activation of AP1 was analyzed by immunoblotting and the phosphorylation of c-Jun was observed significantly less in combined drug treated macrophages comparing to the individual drug treated cells (**Fig. 3.8.2**). This highlights the significant synergistic effect when the antibiotic and the repurposed drug are combined.

Fig. 3.1.8.2: The combined synergistic effect of the antibiotic and the repurposed drug. (A-B) Immunoblot analysis for phospho-c-Jun showing significant decrease in the both drugs treated cells. The experiment was replicated three times individually.

3.1.8.3.Downregulation of p38 activation-

The combined effect of both the antibiotic and the repurposed drug on p38 activation was also evaluated and the same pattern was observed with significant decrease in the phosphorylation of p38 in the combined drugs treated cells (**Fig. 3.1.8.3**). But the significance was that in AP1 activation, there was more decrease in antibiotic treated macrophages than the RD treated cells while in NFkB activation there was more decrease in RD treated cells. So, when we add the effect on both the transcriptional factors, then there is more significant change in the expression of overall transcriptional factors (**Fig. 3.1.8.3C**). This also explains the effectiveness of the combination of both the drugs.
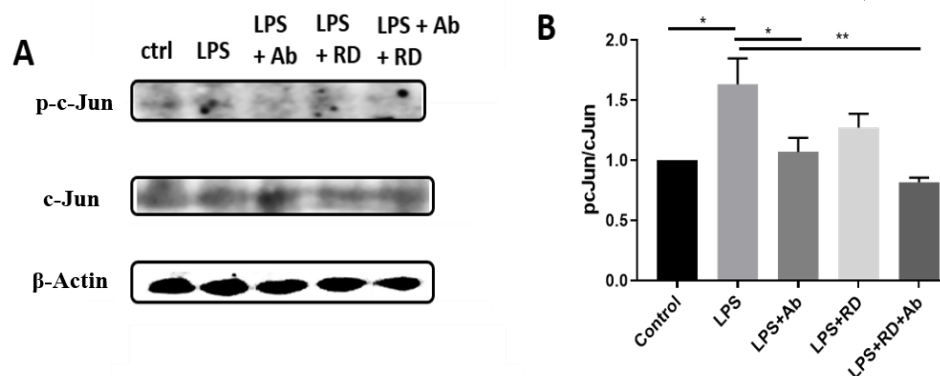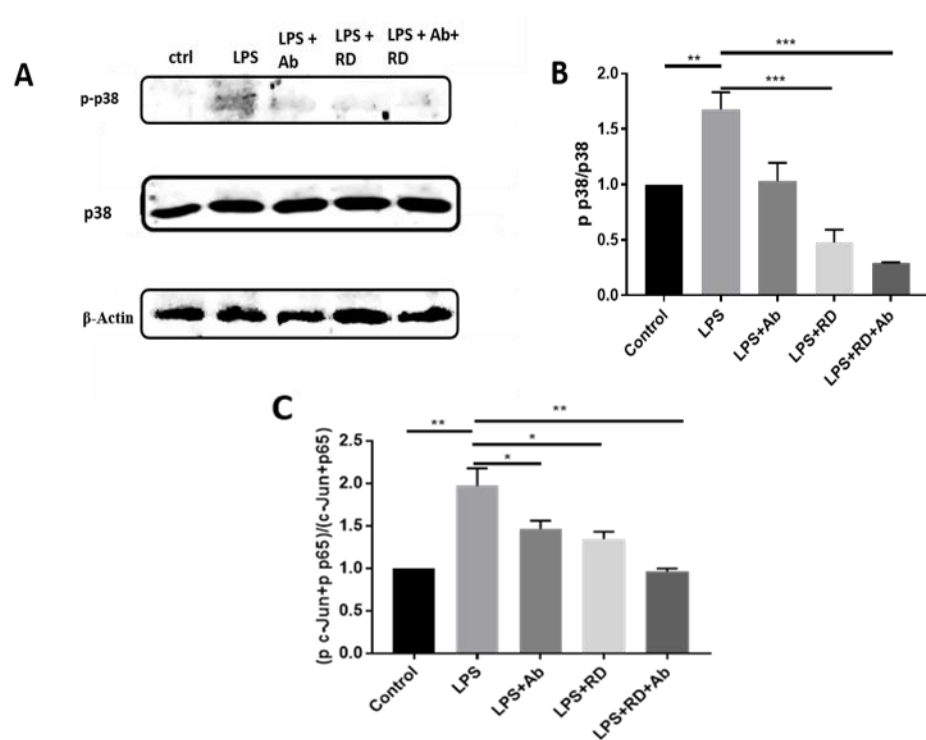
Fig. 3.1.8.3: The combined synergistic effect of the antibiotic and the repurposed drug. (A-B) Immunoblot analysis for phospho-p38 showing significant decrease in the both drugs treated cells, (C) the intensity of p-p65 and p-c-Jun are combined and analyzed for the overall anti-inflammatory effect. The experiment was replicated three times individually.

3.1.9. Synergistic effect of antibiotic and repurposed drug in vivo-

To determine whether the same synergistic effect can be observed in vivo, we treated the septic mice with the individual drugs and the combined drugs. To see if the drugs had the effect on the sepsis affected organs, we collected the major affected organs that were lungs, liver, and kidneys, and analyzed them for the inflammation and necrosis. We also observed the effect of the drugs on the survival of mice which was of prime consideration.

3.1.9.1. Effect of combination on the survival of septic mice-

To determine the effect of the combined synergistic effect on the polymicrobial population induced mice, we prepared five groups of 12 mice each that were untreated, cecal slurry induced septic mice, RD treated septic mice, Ab treated septic mice group, and the combined drugs treated septic mice group. We observed all the groups for 36 hours and found that all mice in septic mice died after 18 hours, in RD treated group all mice died after 22 hours, in Ab treated group 80% mortality was observed after 18 hours, and in combined drugs group 50% mortality was observed after 18 hours and total 75% mortality was observed after 30 hours (**Fig. 3.1.9.1**). Therefore, at 18 hours, there was about 30% more survival in combined drugs group comparing to the only antibiotic group, and 50% more survival than the septic mice group, providing the better efficiency of the combined drugs in treating sepsis than using these drugs individually.
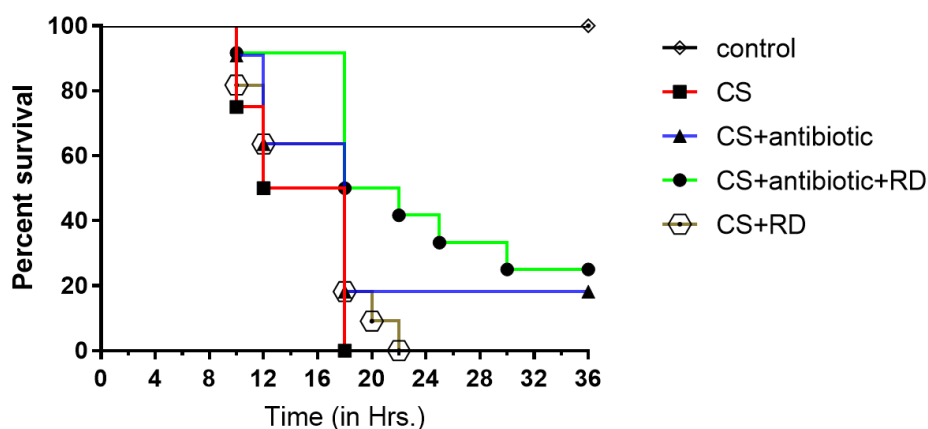
Fig. 3.1.9.1: The survival curve to analyze the efficiency of using drugs in combination to treat sepsis.

3.1.9.2.Effect of combined drugs on various organs of septic mice-

To see the effect of the combined drugs on the various organs of the septic mice, the major affected organs like lungs, liver, and kidneys were collected and were analyzed after H&E-staining. There we found that the immune cells infiltration in each organ were significantly less in the group treated with the drugs in combination and was similar to that of the non-septic mice group. The necrotic area was also found to be less the combined drugs treated group comparing to all the other groups (**Fig. 3.1.9.2A**). We also count the number of immune cells infiltrating in these organs by using ImageJ. There also we observed fewer infiltrating cells in combined drugs treated group (**Fig. 3.1.9.2B**). In conclusion, the drugs when get combined have an anti-inflammatory synergistic effect and more efficiency in treating the life-threatening sepsis condition.
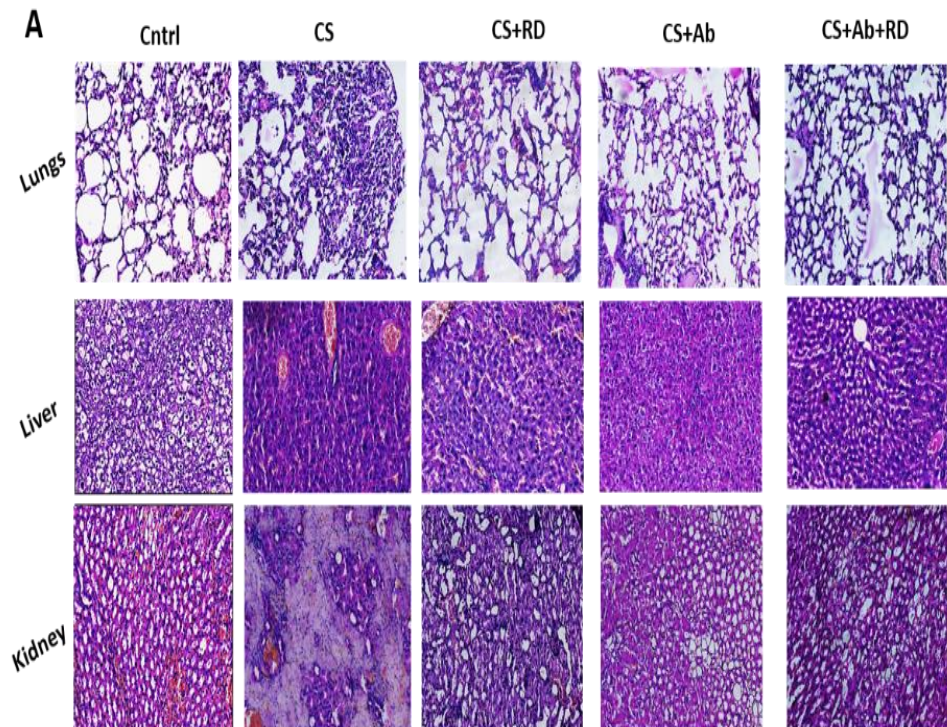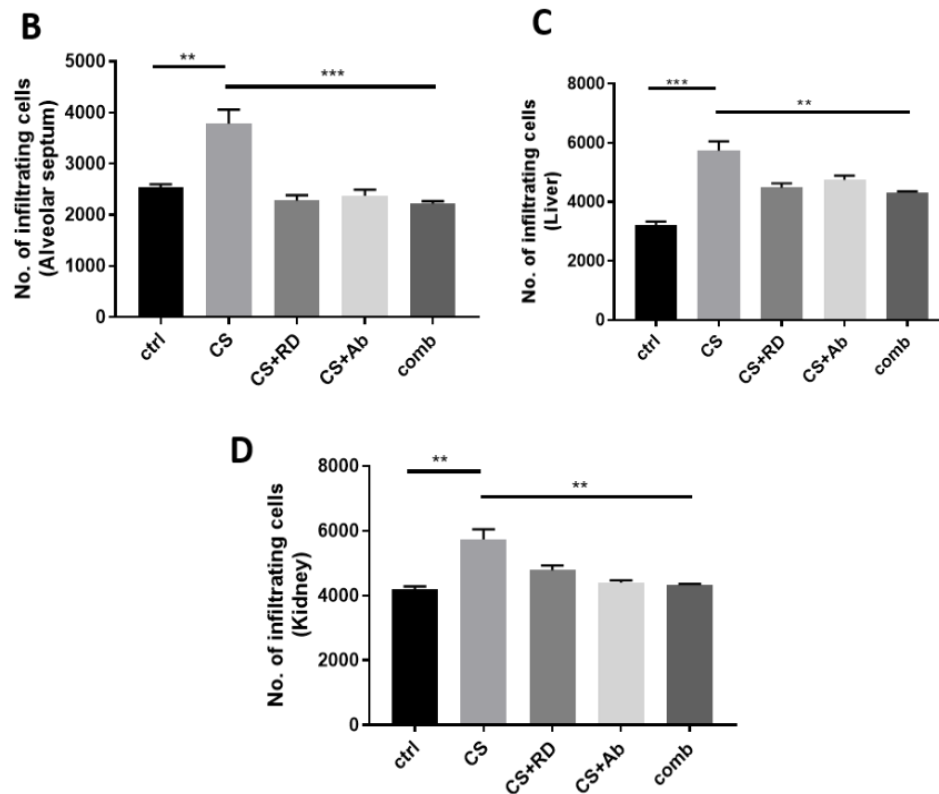
Fig. 3.1.9.2: Tissue section images for lungs, liver, and kidneys. (A) H&E-stained images of the organs from non-treated, cecal slurry induced septic mice group, RD treated mice group, Ab treated group, and combined drugs treated septic mice group. (B-D) Quantification of infiltrating immune cells in alveolar septum, liver, and kidneys, respectively. The experiments were replicated three times individually.

4. Chapter 4

4.1. Conclusion and Future aspects

Sepsis is a multi-organ dysfunction condition which occurs from dysregulated host immune response, majorly mediated by macrophages, after invasion of the pathogens. Currently, the therapeutics on only based on some antibiotics and some anti-endotoxin antibodies, and the mortality rate is still 40-80%. So, there is need of developing a potent therapeutic strategy which can target both the aspects of killing the pathogens as well as the dysregulated host immune response.

This study aims to develop a combination therapy which can meet both the aspects. In this context, we first identified the potent target which can not only induce an efficient anti-inflammatory effect, but also do not take part in normal signaling of the body and we found TIRAP fulfilling all these conditions. Then, we found the site of TIRAP which can be targeted for screening the FDA approved drugs and we found a common site which is binding to BTK, and PKCδ. BTK and PKCδ are involved in activating TIRAP after binding to it and phosphorylating it which then bind to the downstream molecule MyD88. MyD88 further led to activation of two transcriptional factors NFkB and AP1 which are involved in expression of pro-inflammatory cytokines. We got one drug and antibiotic which can efficiently bind to that common interacting site by screening FDA approved library. Further, we validate the anti-inflammatory effect of these computationally screened drugs via in vitro and in vivo studies. We treated the RAW 264.7 mouse macrophages and saw the activation of p65, p38 and AP1 through immunoblotting, immunofluorescence, and RT-PCR techniques. For in vivo studies, we observed the survival of mice and the inflammation in the major affected organs via H&E-staining. From these techniques, we found both the drugs showing the significant anti-inflammatory effect.

Further to check the combined effect of the drugs, there was need of a septic mouse model but the available models were not that much effective due to their certain limitations. Therefore, we report the development of an improved method allowing reproducible and standardized sepsis induction. Our novel approach is based on the intraperitoneal injection of a known amount of enriched polymicrobial population derived from cecum slurry and propagated in LB media until a desired bacterial density, precisely measured by optical density (OD). Herein we proposed the storage of the cultured poly microbiota in glycerol stocks at $-80°C$, allowing us to maintain a constant bacterial population among multiple experiments. The proposed model gives an ethical advantage over previous methods because it avoids unnecessary animal sacrifice for preparing the cecum slurry for each performed experiment.
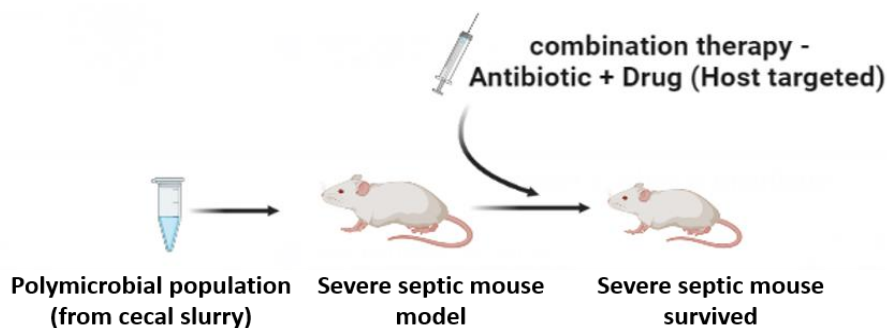
Fig. 4.1: Combination therapy for polymicrobial severe sepsis

On the same septic mouse model, we analyzed the survival and the sepsis characteristics, by treating them with the combined and individual drugs. The survival was observed significantly increased in the combined drugs treated group, and the major organs like lungs, liver, and kidneys were found with less immune cells and less necrotic area indicating the recovery of the organs. In conclusion, the strategy to combine the drugs and getting their synergistic effect is successful and this can be better therapeutic approach to treat the life-threatening sepsis condition. In future, a better combination therapy with more efficacy can be developed by considering the various aspects mentioned in this study.

5. Annexure

5.1. List of primers

Table 5.1: Primer sets used for RT-PCR.

S.No.	Gene target	Sequence (5'-3')
1.	GAPDH (F)	AACTTTGGCATTGTGGA AGG
2.	GAPDH (R)	CACATTGGGGGTAGGAA CAC
3.	IL-12 (F)	TCGCAGCAAAGCAAGATGTG
4.	IL-12 (R)	GAGCAGCAGATGTGAGTGGC
5.	IL-23 (F)	ACCAGCGGGACATATGAATCT
6.	IL-23 (R)	AGACCTTGGCGGATCCTTTG

5.2. List of antibodies

Table 5.2: Antibodies used for immunoblotting and immunofluorescence.

S.No.	Antibody	Cat. No.	Dilution used for immune-fluorescence	Dilution used for immunoblot
1.	p-p65	CS-3033	-----	(1:1,000)
2.	p65	Sc-8008	(1:200)	(1:1,000)
3.	p-TIRAP	BS-756R	-----	(1:1,000)
4.	TIRAP	13077S	-----	(1:1,000)
5.	p-p38	SC 17852-R	-----	(1:1,000)
6.	p38	SC7972	-----	(1:1,000)
7.	p-c-Jun	SC822	-----	(1:1,000)
8.	c-Jun	SC74543	-----	(1:1,000)

9.	Actin	Sc-47778	-----	(1:1,000)
10.	Anti-Rabbit HRP	65-6120	-----	(1:5,000)
11.	Anti-Mouse HRP	Sc-2318	-----	(1:10,000)
12.	Anti-Mouse FITC	Novex-A16018	(1:600)	-----
13.	Anti-Rabbit AF594	A11012	(1:600)	-----

6. REFERENCES

Angus, D. C., & van der Poll, T. (2013). Severe Sepsis and Septic Shock. *New England Journal of Medicine*, *369*(9), 840–851. https://doi.org/10.1056/NEJMra1208623

Atre, R., Sharma, R., Obukhov, A. G., Saqib, U., Umar, S., Darwhekar, G. N., & Baig, M. S. (2023). *An improved mouse model of sepsis based on intraperitoneal injections of the enriched culture of cecum slurry* [Preprint]. Immunology. https://doi.org/10.1101/2023.04.06.535817

Bernard, A. M., & Bernard, G. R. (2012). The Immune Response: Targets for the Treatment of Severe Sepsis. *International Journal of Inflammation*, *2012*, 1–9. https://doi.org/10.1155/2012/697592

Bosmann, M., & Ward, P. A. (2013). The inflammatory response in sepsis. *Trends in Immunology*, *34*(3), 129–136. https://doi.org/10.1016/j.it.2012.09.004

bradley, P. (2023). *Thiamine and High Dose Insulin Treatment for Sepsis* [Preprint]. Medicine and Pharmacology. https://doi.org/10.20944/preprints202304.0796.v1

Dorofeyeva, L. V. (1975). Obtaining of measles virus haemagglutinin from strain L-16 grown in primary cell cultures. *Acta Virologica*, *19*(6), 497.

Gardos, G., & Cole, J. O. (1976). Maintenance antipsychotic therapy: Is the cure worse than the disease? *The American Journal of Psychiatry*, *133*(1), 32–36. https://doi.org/10.1176/ajp.133.1.32

Iscimen, R., Cartin-Ceba, R., Yilmaz, M., Khan, H., Hubmayr, R. D., Afessa, B., & Gajic, O. (2008). Risk factors for the development of

acute lung injury in patients with septic shock: An observational cohort study*: *Critical Care Medicine*, *36*(5), 1518–1522. https://doi.org/10.1097/CCM.0b013e31816fc2c0

Jarczak, D., Kluge, S., & Nierhaus, A. (2021a). Sepsis—Pathophysiology and Therapeutic Concepts. *Frontiers in Medicine*, *8*, 628302. https://doi.org/10.3389/fmed.2021.628302

Jarczak, D., Kluge, S., & Nierhaus, A. (2021b). Sepsis—Pathophysiology and Therapeutic Concepts. *Frontiers in Medicine*, *8*, 628302. https://doi.org/10.3389/fmed.2021.628302

Parry, W. H., Martorano, F., & Cotton, E. K. (1976a). Management of life-threatening asthma with intravenous isoproterenol infusions. *American Journal of Diseases of Children (1960)*, *130*(1), 39–42. https://doi.org/10.1001/archpedi.1976.02120020041006

Parry, W. H., Martorano, F., & Cotton, E. K. (1976b). Management of life-threatening asthma with intravenous isoproterenol infusions. *American Journal of Diseases of Children (1960)*, *130*(1), 39–42. https://doi.org/10.1001/archpedi.1976.02120020041006

Parry, W. H., Martorano, F., & Cotton, E. K. (1976c). Management of life-threatening asthma with intravenous isoproterenol infusions. *American Journal of Diseases of Children (1960)*, *130*(1), 39–42. https://doi.org/10.1001/archpedi.1976.02120020041006

Polat, G., Ugan, R. A., Cadirci, E., & Halici, Z. (2017a). Sepsis and Septic Shock: Current Treatment Strategies and New Approaches. *The Eurasian Journal of Medicine*, *49*(1), 53–58. https://doi.org/10.5152/eurasianjmed.2017.17062

Polat, G., Ugan, R. A., Cadirci, E., & Halici, Z. (2017b). Sepsis and Septic Shock: Current Treatment Strategies and New Approaches. *The Eurasian Journal of Medicine*, *49*(1), 53–58. https://doi.org/10.5152/eurasianjmed.2017.17062

Polat, G., Ugan, R. A., Cadirci, E., & Halici, Z. (2017c). Sepsis and Septic Shock: Current Treatment Strategies and New Approaches. *The

Eurasian Journal of Medicine, *49*(1), 53–58.
https://doi.org/10.5152/eurasianjmed.2017.17062

Rajpoot, S., Srivastava, G., Siddiqi, M. I., Saqib, U., Parihar, S. P., Hirani,
N., & Baig, M. S. (2022). Identification of novel inhibitors targeting
TIRAP interactions with BTK and PKCδ in inflammation through
an in silico approach. *SAR and QSAR in Environmental Research*,
33(3), 141–166. https://doi.org/10.1080/1062936X.2022.2035817

Rajpoot, S., Wary, K. K., Ibbott, R., Liu, D., Saqib, U., Thurston, T. L. M.,
& Baig, M. S. (2021a). TIRAP in the Mechanism of Inflammation.
Frontiers in Immunology, *12*, 697588.
https://doi.org/10.3389/fimmu.2021.697588

Rajpoot, S., Wary, K. K., Ibbott, R., Liu, D., Saqib, U., Thurston, T. L. M.,
& Baig, M. S. (2021b). TIRAP in the Mechanism of Inflammation.
Frontiers in Immunology, *12*, 697588.
https://doi.org/10.3389/fimmu.2021.697588

Rudd, K. E., Johnson, S. C., Agesa, K. M., Shackelford, K. A., Tsoi, D.,
Kievlan, D. R., Colombara, D. V., Ikuta, K. S., Kissoon, N., Finfer,
S., Fleischmann-Struzek, C., Machado, F. R., Reinhart, K. K.,
Rowan, K., Seymour, C. W., Watson, R. S., West, T. E., Marinho,
F., Hay, S. I., … Naghavi, M. (2020). Global, regional, and national
sepsis incidence and mortality, 1990–2017: Analysis for the Global
Burden of Disease Study. *The Lancet*, *395*(10219), 200–211.
https://doi.org/10.1016/S0140-6736(19)32989-7

Shalova, I. N., Lim, J. Y., Chittezhath, M., Zinkernagel, A. S., Beasley, F.,
Hernández-Jiménez, E., Toledano, V., Cubillos-Zapata, C.,
Rapisarda, A., Chen, J., Duan, K., Yang, H., Poidinger, M., Melillo,
G., Nizet, V., Arnalich, F., López-Collazo, E., & Biswas, S. K.
(2015). Human Monocytes Undergo Functional Re-programming
during Sepsis Mediated by Hypoxia-Inducible Factor-1α. *Immunity*,
42(3), 484–498. https://doi.org/10.1016/j.immuni.2015.02.001

Share, J. B. (1976a). Review of drug treatment for Down's syndrome persons. *American Journal of Mental Deficiency*, *80*(4), 388–393.

Share, J. B. (1976b). Review of drug treatment for Down's syndrome persons. *American Journal of Mental Deficiency*, *80*(4), 388–393.

Singer, M., Deutschman, C. S., Seymour, C. W., Shankar-Hari, M., Annane, D., Bauer, M., Bellomo, R., Bernard, G. R., Chiche, J.-D., Coopersmith, C. M., Hotchkiss, R. S., Levy, M. M., Marshall, J. C., Martin, G. S., Opal, S. M., Rubenfeld, G. D., van der Poll, T., Vincent, J.-L., & Angus, D. C. (2016). The Third International Consensus Definitions for Sepsis and Septic Shock (Sepsis-3). *JAMA*, *315*(8), 801. https://doi.org/10.1001/jama.2016.0287

Towbin, H. (2009). Origins of protein blotting. Protein Blotting and Detection, Springer: 1-3. (n.d.).

Vincent, J.-L., Jones, G., David, S., Olariu, E., & Cadwell, K. K. (2019a). Frequency and mortality of septic shock in Europe and North America: A systematic review and meta-analysis. *Critical Care*, *23*(1), 196. https://doi.org/10.1186/s13054-019-2478-6

Vincent, J.-L., Jones, G., David, S., Olariu, E., & Cadwell, K. K. (2019b). Frequency and mortality of septic shock in Europe and North America: A systematic review and meta-analysis. *Critical Care*, *23*(1), 196. https://doi.org/10.1186/s13054-019-2478-6

Ward, P. A., & Gao, H. (2009). Sepsis, complement and the dysregulated inflammatory response. *Journal of Cellular and Molecular Medicine*, *13*(10), 4154–4160. https://doi.org/10.1111/j.1582-4934.2009.00893.x